RSC Advances

ROYAL SOCIETY OF CHEMISTRY

www.rsc.org/advances

Bio:

Han Gao is pursuing his PhD degree in the Department of Materials Science and Engineering , University of Toronto. After obtaining a B.A.Sc degree (hons.) in 2010, he joined the Flexible Energy and Electronics Laboratory under the guidance of Prof. Keryn Lian. His research is on the design, synthesis, and fundamental studies of advanced polymer electrolyte systems for energy storage systems, such as supercapacitors. He has won several awards including a 1st prize in the student poster competition at the 2011 Fall Symposium of the Electrochemical Society Canadian Section and is a recipient of multiple scholarships from provincial to national.

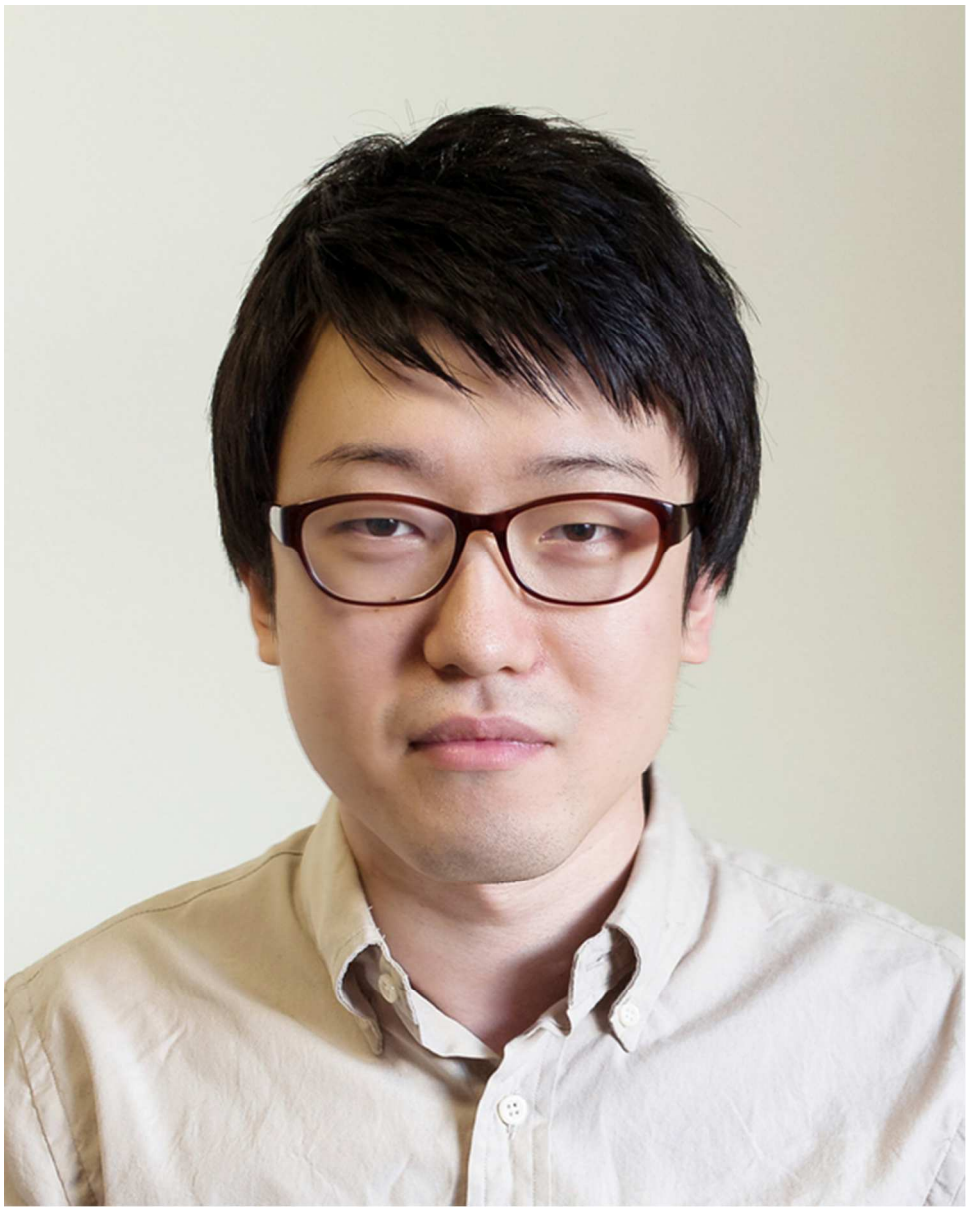

Photo of H.Gao
49x62mm (300 x 300 DPI)

Keryn Lian is Associate Professor of Materials Science and Engineering at the University of Toronto. Her research interests are novel materials that enable light-weight, thin, and flexible energy storage. Her group has developed advanced pseudocapacitive materials to modify carbon electrodes; high performance proton-conducting, hydroxide ion-conducting, and ionic liquid-conducting polymer electrolytes; and leveraged these in electrochemical capacitors. Prior to joining UofT, she conducted and led research at Motorola Labs in energy storage, RF-MEMS, and microfluidics, leading to advanced printed wiring board technologies. She has published over 80 papers in refereed journals and conference proceedings, and holds 35 issued US patents.

photo of K.Lian
127x158mm (600 x 600 DPI)

Proton-Conducting Polymer Electrolytes and Their Applications in Solid Supercapacitors: A Review

Han Gao and Keryn Lian*

Department of Materials Science and Engineering, University of Toronto, Toronto, Ontario, Canada M5S 3E4

* E-mail: keryn.lian@utoronto.ca

Contents

Abstract

Research on solid supercapacitors over the last few years has aimed to provide high performing and safely operating energy storage solutions for the fast growing application areas of consumer and micro-electronics, providing printable, flexible and wearable devices. Most of the reported research has leveraged proton conducting polymer electrolytes for electrochemical double layer capacitors and pseudo-capacitors. In this paper, we provide an overview of the state-of-the-art solid supercapacitors enabled by proton-conducting polymer electrolytes. After a short overview of the types and configurations of solid supercapacitors, this review introduces proton-conducting polymers electrolytes and the mechanisms of proton conduction in a polymer matrix. Based on their chemistry, synthesizing method, and the nature of proton conduction, proton-conducting polymer electrolytes and the resultant supercapacitors are discussed in two categories: polymeric proton-conducting electrolytes and inorganic/polymer proton-conducting electrolytes. The performance and the technology gaps of the solid supercapacitors enabled by the presented polymer electrolytes are reviewed and compared. The review concludes with an outlook of future advancements required and the key research directions to achieving these.

1 Solid supercapacitors

Supercapacitors are electrochemical energy storage devices that can stand alone or complement batteries in hybrid systems to reach high power density and fast charge/ discharge rates.[1-7] In contrast to batteries, they have a much longer service life and

excellent cycling capability without losing their energy storage capacity. In industrial and automotive applications, supercapacitors mainly provide regenerative power and peak assist, while in consumer electronics, they are much smaller and can supplement or replace batteries. Yet smaller supercapacitors, often referred to as micro-supercapacitors, have emerged for on-chip applications such as powering micro-electromechanical systems (MEMS) and bio-sensors.[8] In addition, some high rate micro-supercapacitors have shown potential to replace electrolytic capacitors for alternating current line filtering with very small RC (resistor-capacitor) time constants.[9]

Supercapacitors can be categorized along various criteria as shown in Fig. 1. Depending on the charge storage mechanism, supercapacitors can be divided into electrochemical double layer capacitors (EDLCs) and pseudo-capacitors. While EDLCs store charge electrostatically at the electrode/electrolyte interface as charge separation, pseudo-capacitors store energy by charge transfer between electrode and electrolyte via Faradaic reactions. Supercapacitors come in either symmetric (using electrodes with the same capacitance) or asymmetric (using electrodes with different capacitance) configurations. Asymmetric supercapacitors may consist of a double layer electrode and a pseudo-capacitive electrode or two different pseudo-capacitive electrodes.

In a traditional supercapacitor, an ion-permeable and electrically insulating separator film is sandwiched between two electrodes flooded with a liquid electrolyte. Since liquid electrolyte leakage is a severe issue, especially when the material is environmentally hazardous, efforts abound to replace liquid electrolytes with solid electrolytes for next generation solid supercapacitors that are not only safer, but also offer high performance, light weight, and flexible form factors.

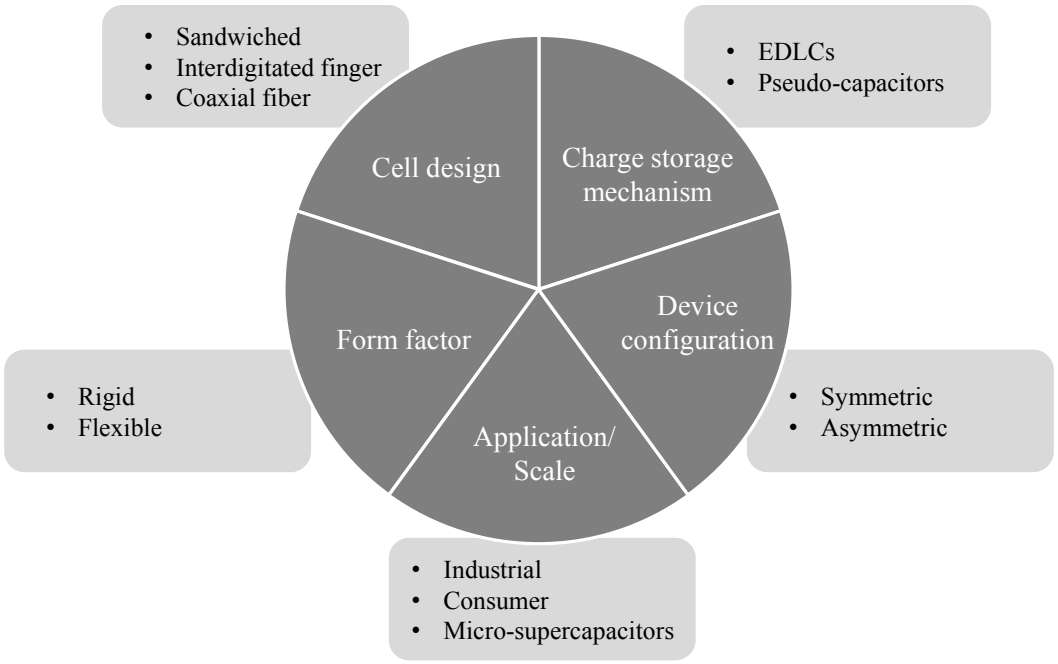

Fig. 1 Classifications of supercapacitors.

Solid supercapacitors are mainly targeting consumer electronics, micro-electronics, and wearable or printable electronics. Thin and lightweight electronics or micro-electronics, including micro-robots, implantable medical devices, sensors, and smart cards, require flexible power sources with smaller dimensions and higher power density. In recent years, significant efforts have been dedicated to achieving thin and/or free-standing supercapacitor electrodes, including carbon nanotube (CNT) films, graphene sheets, reduced graphene oxide, conducting polymer/carbon composites, or metal oxide/carbon composites.[10-12] At the same time, flexible substrates or supports have been investigated for solid supercapacitors, including paper, textile, woven cotton, and fabrics.[13] Although these materials have led to an advance in flexible solid supercapacitors, the commercialization of such devices still remains challenging. One of the main limitations is the availability of solid electrolytes.

Among solid electrolytes, polymer electrolytes are ideal candidates for flexible solid supercapacitors. A polymer electrolyte can enable different supercapacitor cell designs with minimum packaging (see Fig. 2). Slim supercapacitor multi-cell modules can be constructed by inserting bi-polar electrodes between terminal electrodes and electrolyte layers in a sandwiched cell. The thickness of both the electrode and the polymer electrolyte affects the equivalent series resistance (ESR) and rate performance of such supercapacitors. In contrast, in an interdigitated finger structure or in a coaxial structure, the electrolyte resistance dominates the cell ESR and the rate capability.

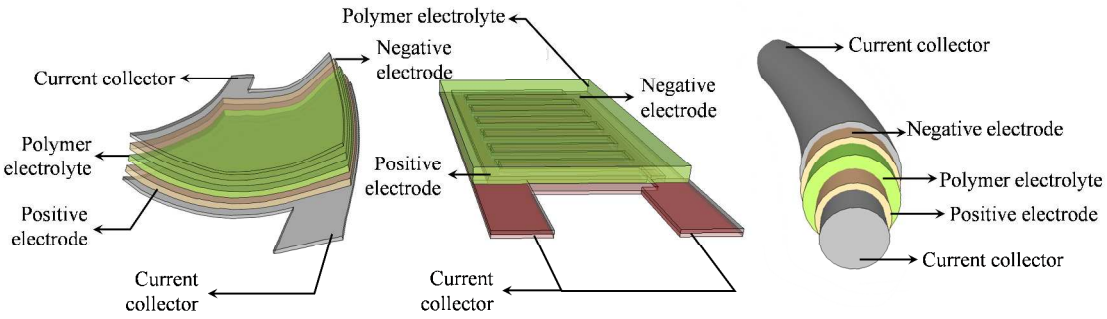

Fig. 2 Schematic of polymer electrolyte-enabled supercapacitors in flexible sandwiched cell configuration (left), interdigitated finger cell configuration (middle), and coaxial fiber cell configuration (right).

Traditionally, a polymer electrolyte is produced as a free-standing film which enables a flexible sandwiched cell design. A polymer electrolyte can also be prepared in the form of a precursor solution, where the electrodes are either immersed in the polymer electrolyte solution or the electrolyte solution is cast on the electrode, followed by drying and pressing for cell assembly. The polymer electrolyte precursor solution can impregnate the active layer of the supercapacitor electrodes, thereby increasing the electrochemically active surface area. Through pressing, the resultant thin polymer electrolyte layers on both electrode surfaces are integrated into a single thin layer minimizing interfacial resistance.

For supercapacitor applications, proton-conducting polymer electrolytes are of special interest since they tend to have high ionic conductivity and many pseudo-capacitive electrodes require protons for their Faradaic redox reactions. To date, proton-conducting polymer electrolytes for solid supercapacitor applications have not been discussed extensively albeit they are widely used (and reviewed) for fuel cells. A major difference between proton-conducting polymer electrolytes in fuel cells and supercapacitors is their application temperature, as the latter are normally operated under ambient conditions and sometimes, at low temperatures. This review explores the state-of-the-art research on low to room temperature proton-conducting polymer electrolytes, with a particular emphasis on polymeric proton-conducting and inorganic/polymer proton-conducting electrolytes. Section 2 introduces proton-conducting polymer electrolytes and discusses the mechanisms of proton conduction. In Sections 3 and 4, we review the development of proton-conducting polymer electrolytes and the performance of supercapacitors enabled by these electrolytes. The focus of our comparison is on the chemistries and production processes of the electrolytes and their contributions to device performance. New trends in material development are identified and key research results are summarized in tabular form, highlighting the particular polymer electrolytes developed, their proton conductivity, and processing method as well as the cell design, electrode material, testing conditions, and achieved capacitance for the supercapacitors. The performance of enabled supercapacitors is typically compared to a cell using a liquid H_2SO_4 electrolyte. For brevity, we shall refer to such device as “liquid cell”. Finally, Section 5 presents challenges faced in the development and deployment of solid polymer electrolytes for supercapacitor applications.

Unlike conventional supercapacitors with liquid electrolytes, where performance is often reported based on gravimetric values, for solid supercapacitors (especially flexible devices), the performance should be normalized by volume or geometric area instead of the mass of the active material.[14] Since the weight of the active electrode materials (typically only a few micrometers or even nanometers thick) is almost negligible compared to the other components in a thin film device, gravimetric values will result in an unreliable and even unfair comparison of device performance. Unfortunately, the majority of the literature reports gravimetric values of active materials only and these are reflected in the comparison of the chemistries of the polymer electrolytes presented below. In addition, the reported cell capacitance varies widely as it is highly dependent on the electrode materials.

2 Proton-conducting polymer electrolytes

For solid supercapacitor applications, polymer electrolytes should exhibit the following properties: (i) high ionic conductivity at room temperature; (ii) low electronic conductivity; (iii) good mechanical properties or dimensional stability; (iv) high chemical, electrochemical, and environmental stability; and (v) sufficient thin-film processability. Most polymer electrolytes conduct via the movement of protons, lithium ions,[15, 16] hydroxide ions[17, 18] or the ionic species in ionic liquids.[19-23] The conduction mechanism should match the chemistry of the electrodes in order to form a device. Among these electrolytes, proton- and lithium ion-conducting polymer electrolytes are the most mature. Lithium-conducting polymer electrolytes are adapted from lithium-ion batteries and include various lithium salts dissolved in organic solvents and immobilized in a polymer matrix[15] and solid-state lithium ion conductors.[16] While they possess a wide

electrochemical window, these electrolytes generally exhibit limited ionic conductivity. In addition, they are moisture sensitive and thus require an oxygen-free environment for cell assembly. Proton-conducting polymer electrolytes, inspired by fuel cells, have the highest ionic conductivity among all polymer electrolytes. Their main drawback is their narrower voltage window. They can be processed and utilized under ambient conditions, but as proton conducting polymer electrolytes rely on the presence of water to achieve high proton conductivity, maintaining a high degree of hydration at room temperature or lower is critical to achieve high performance.

The study of proton conduction in solids started with the fact that ice conducts electricity.[24, 25] Subsequently, the study of proton-conducting materials and the investigation of proton conductivity expanded to proton-conducting polymer electrolytes for applications below the boiling point of water and proton-conducting oxides for higher temperature applications. Table 1 summarizes the brief history of both polymeric and inorganic proton-conducting materials as well as their application ranges.

Table 1 Brief history of polymeric and inorganic proton-conducting materials.

Year	Material	Application temperature	Reference
1806	Aqueous solutions	<100 °C	26
1877	Ice	<0 °C	24, 25
1920s	Zeolites	<100 °C	27
1930s	Hydrogen uranyl phosphate (HUP)	100-400 °C	28
1960s	Nafion®	<100 °C	29, 30
1970s	$MHSO_4$, where M=Cs, Rb	>100 °C	31
1970s	Zirconium hydrogenphosphate ($Zr(HPO_4)_2$)	200-350 °C	32
1970s	β- and β”-alumina	100-300 °C	33
1980s	Perovskite type oxides	>300 °C	27
1980s	Acid/polymer blends (e.g. H_2SO_4/PVA)	<100 °C	34-36
1980s	Heteropolyacids (e.g. $H_4SiW_{12}O_{40}$)	<200 °C	37
1990s	Oxide gels	<100 °C	38
1990s	Aromatic ionomers	>100 °C	39

Proton conduction can be observed in many materials, from rigid inorganic oxides at high temperatures to flexible organic polymers at room temperature, leveraging different conduction mechanisms. Depending on the type of proton conductor, proton-conducting polymer electrolytes can be classified into different groups, as shown in Fig. 3. Polymeric proton-conducting electrolytes possess "intrinsic" proton conductivity from the functional group in the polymer chains, whereas the inorganic/polymer proton-conducting electrolytes blend inorganic proton conductors with a polymeric matrix to form gels or composites.

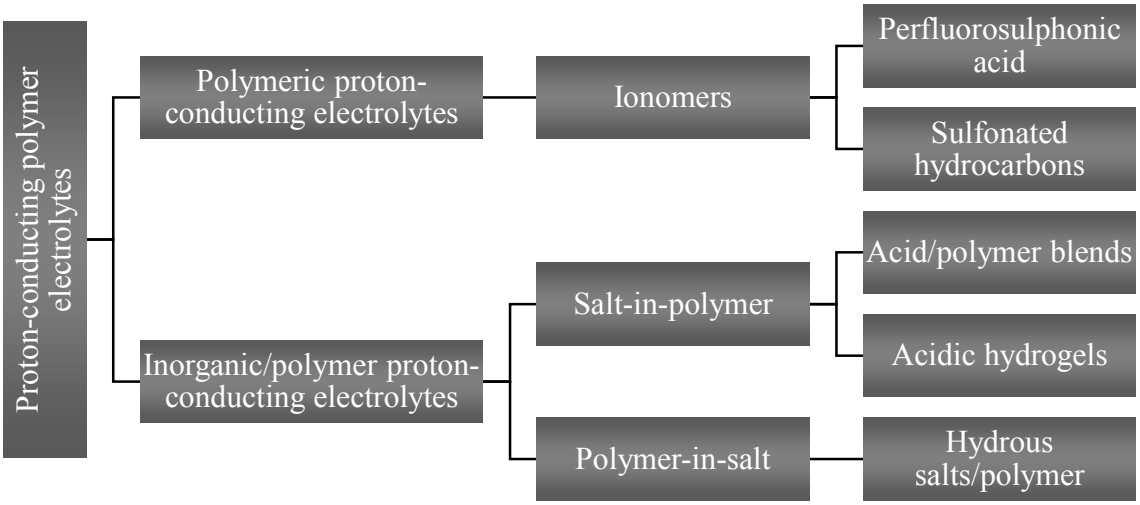

Fig. 3 Categories of low to room temperature proton-conducting polymer electrolytes depending on the nature of the ionic conductor.

Most proton-conducting materials have been extensively studied for fuel cell applications. However due to the higher operating temperature of fuel cells compared to supercapacitors, the development of low to room temperature proton-conducting polymer electrolytes has been limited. In order to design and optimize suitable proton-conductors as electrolytes for solid supercapacitors, it is essential to understand the proton migration

mechanisms below or at room temperature. The proton transport in polymer electrolytes can be described based on three main mechanisms, as shown in Fig. 4: (a) proton hopping or Grotthuss mechanism; (b) diffusion or vehicle mechanism; and (c) direct transport via polymer chain segmental motions.[40-42]

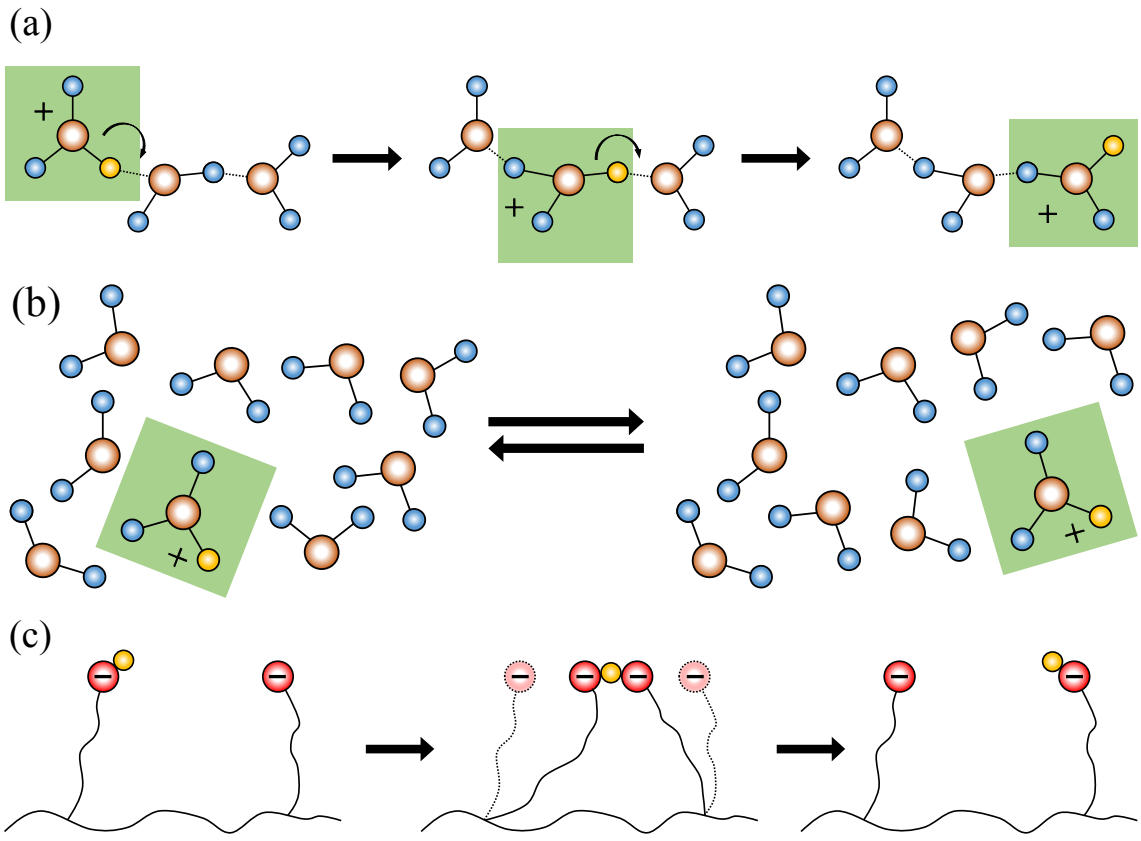

Fig. 4 Schematic of low temperature proton transport mechanisms: (a) hopping or Grotthuss mechanism in a system with strong hydrogen bonding; (b) diffusion or vehicle mechanism in a system with weak hydrogen bonding; and (c) direct transport via polymer chain segmental motions.

Under the Grotthuss mechanism, the mobility of protons is determined by the formation or cleavage rate of the hydrogen bond between a hydronium ion (which itself can be hydrated in the form of $H_5O_2^+$, $H_7O_3^+$, $H_9O_4^+$, etc.) and a water molecule or other hydrogen-bonded liquids.[42, 43] Protons "hop" from one hydrolyzed ionic site to another (Fig. 4a). Site-to-site hopping between different sites with local rearrangement and

reorientation is characterized by two potential wells, corresponding to the proton donor and the proton acceptor. The potential wells are separated by a potential barrier of a few $kJmol^{-1}$. This low activation energy together with the high proton mobility of the proton hopping mechanism occurs primarily in a system with strong hydrogen bonding.[41, 44]

Under the diffusion mechanism, a proton combines with solvent molecules (e.g. water), producing a complex and then diffuses.[44] As shown in Fig. 4b, a proton can be transferred by the diffusion of hydrogen-water ions (H_3O^+ in this example). The diffusion process is driven by a gradient in proton concentration. Diffusion of the hydrogen-water ions may decrease due to hydrogen bonding with other water molecules. The diffusion process is much slower than proton hopping and is characterized by a higher activation energy and lower proton mobility.

Proton mobility can also result from segmental motions of the polymer chains (Fig. 4c). However, this type of proton transportation is restricted to the amorphous phase of the solvating polymers, where the polymer molecules are free to move. Therefore, proton conduction by segmental motion is only possible above the glass transition temperature (T_g) of the polymer. In the amorphous phase, the polymer side chains can vibrate to a certain extent, thus reducing or eliminating the distance for proton conduction.

To investigate the proton conduction mechanism, proton conductivity (σ) is typically characterized as a function of temperature (T). In an Arrhenius plot, the logarithm of the proton conductivity is graphed against the inverse of the temperature. A straight line indicates an Arrhenius type temperature dependence, while a curved line can be empirically fitted using Vögel-Tamman-Fulcher (VTF) equations.[45] The activation energy can be evaluated from the slope of the $\ln(\sigma)$ *vs.* (1000/T) plots.

In order to reach high proton conductivity in polymer electrolytes, a high degree of hydration is essential, as proton conductivity increases with temperature and relative humidity (RH). At a constant temperature, protons are transported via the Grotthuss mechanism with high mobility at high RH and via the vehicle mechanism with lower mobility at low RH. In contrast, with increasing temperature, the vehicle mechanism progressively dominates the Grotthuss mechanism, as hydrogen bonds begin to elongate and break.

3 Polymeric proton-conducting electrolytes and enabled supercapacitors

Polymeric proton-conducting electrolytes have been intensively studied for electrochemical energy storage devices. Of main interest are pure ionomers containing negatively charged functional sites (mainly $–SO_3H$, $-PO_4H_2$, -COOH), due to their higher proton conductivity below 100 °C. These polymer electrolytes typically have a multiphase structure containing both hydrophobic and hydrophilic regions. The charge from the fixed functional sites can be compensated for by mobile protons exchanged within the media. While in fuel cell applications we also find polymer films soaked with phosphoric acid, e.g. polybenzimidazole (PBI)-H_3PO_4, and pure ionomers soaked with ionic liquids, these electrolytes have no application in room temperature supercapacitors.

3.1 Perfluorosulphonic acid electrolytes

Among polymeric proton-conducting electrolytes, perfluorosulphonic acid (PFSA) membranes have emerged as materials of choice for low temperature applications requiring high stability and chemical resistance. One of the most well-known PFSAs is

Nafion®, which has been the gold standard proton-conducting polymer electrolyte for decades.[46-48] By combining the extreme hydrophobicity of the polytetrafluorethylene (PTFE) backbone with perfluorinated side chains and terminated by sulfonic acid ($-SO_3H$) groups in Nafion, strong hydration (solvation) can occur and lead to complete proton dissociation. Water not only dissociates the protons from the acid groups, but also facilitates the mobility of hydrated protons via Grotthuss and vehicle mechanisms.

The water molecules are only loosely bonded to the hydrophilic $-SO_3H$ groups and can be readily removed in low RH, causing a high energy barrier for proton transport and low proton conductivity. As a result, the proton conduction mechanism is highly dependent on the hydration state of the polymer electrolyte. The proton conductivity of different Nafion films has been characterized extensively as a function of temperature and RH.[46, 47] For example, Maréchal *et al.* have investigated the proton conductivity of Nafion-117 under different temperatures and RH and observed that the proton transport in Nafion-117 is highly sensitive to temperature and to the level of hydration in the membrane.[46] In spite of the sensitivity to dehydration, the success and maturity of PFSAs in fuel cells has made them a preferred choice for both EDLC and pseudo-capacitors as summarized in Tables 2 and 3, respectively.

3.1.1 Electrochemical double layer capacitors

Staiti *et al.* demonstrated the first all solid EDLC using a Nafion ionomer solution and carbon electrodes.[49, 50] Both a commercial Nafion-115 membrane and a solution-casted Nafion-1100 film were investigated. The EDLC assembled with the casted Nafion membrane exhibited higher performance but its capacitance was lower than that of a liquid cell. An enhancement in cell capacitance was obtained by introducing a

homogeneous inter-distributed Nafion solution into the carbon electrodes yielding improved adhesion between electrodes and the electrolyte.[51] Fast proton transport was confirmed in smaller carbon pores due to the presence of water in the Nafion solution. The cyclic voltammograms (CV) for the solid Nafion capacitor and the liquid cell were comparable; both exhibited a rectangular CV profile and almost equivalent capacitance.

To demonstrate the feasibility of scaling up Nafion polymer electrolyte-enabled solid EDLCs, a multi-cell prototype was constructed by stacking five single solid cells.[52] This device reached 1.5 F capacitance with 5 V working voltage and a 0.3 s RC time constant. Studies of the performance of EDLCs based on Nafion in various forms (i.e. H^+, Na^+, and K^+) observed an increase in specific capacitance in the order of $H^+ < Na^+ < K^+$ due to an increase in the charge carrying capacity.[53] Since the use of pure Nafion is not economical, Subramaniam *et al.* investigated solid EDLCs based on composites of Nafion with PTFE or cellulose acetate.[54] The membranes were prepared by soaking PTFE or cellulose acetate in a Nafion solution followed by drying in a vacuum oven. Improvements in the mechanical strength of the solid electrolyte in the dry state and in the dimensional stability in the hydrated state were observed. However, both Nafion/PTFE and Nafion/cellulose acetate composite polymer electrolyte films suffered from a substantial loss of proton conductivity.

To facilitate charge and ion transport at the electrode/electrolyte interface for EDLCs, Choi *et al.* prepared flexible solid EDLCs by slowly pouring a Nafion solution onto the thin film electrode.[55] This electrode/electrolyte integration promoted interconnected network structures at the interface, resulting in a two-fold increase in capacitance compared to the EDLC without Nafion integration (118.5 Fg^{-1} vs. 62.3 Fg^{-1} at

1 Ag^{-1}, as shown in Fig. 5). Similarly, Huang *et al.* assembled a flexible solid EDLC by spraying aqueous suspensions of multi-wall carbon nanotubes (MWNTs) in a Nafion ionomer solution and an H_2SO_4 solution directly onto both sides of a Nafion membrane.[56] The Nafion and H_2SO_4 solutions ensured better proton penetration into the interior of the electrodes, promoting electrolyte wetting and ion adsorption, and consequentially higher cell capacitance and proton mobility. A 3 V EDLC device was demonstrated by connecting the flexible cells in series. Relying on the same concept, Cole *et al.* built Nafion-based stretchable solid EDLCs using aligned CNTs, which reached a capacitance of 72 Fg^{-1} after soaking in 1 M H_2SO_4 for polymer electrolyte hydration.[57]

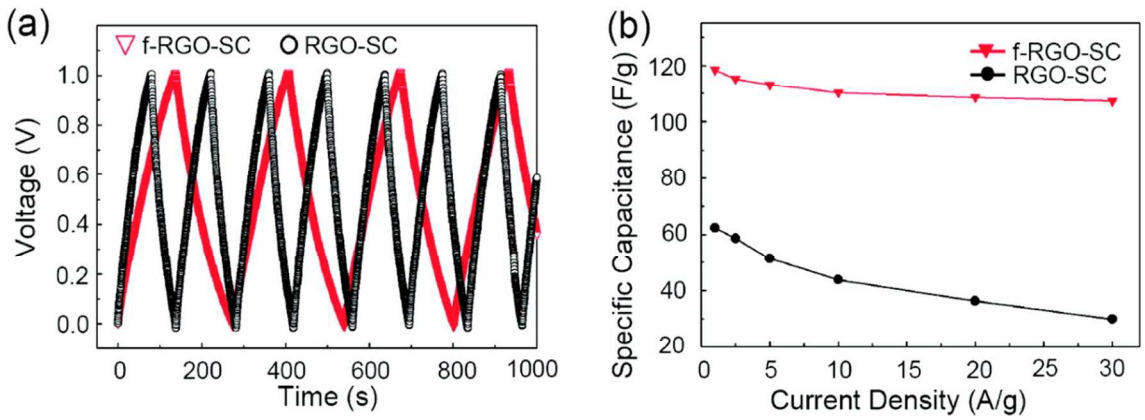

Fig. 5 (a) Charge/discharge curves under a current density of 1 A/g for supercapacitors with (f-RGO-SC) and without (RGO-SC) Nafion integration; and (b) specific capacitance of the two supercapacitors as a function of current density. Reprinted with permission from Choi *et al.*[55] Copyright 2011 American Chemical Society.

Table 2 Summary of PFSA solid EDLCs reported in the literature.

Polymer electrolyte	Proton conductivity (Scm^{-1})	Electrolyte production method	Cell design	Testing/storage environment	Electrode active material	Cell capacitance	Ref.
Nafion-115[a]	5.7×10^{-2}	Free-standing film	Sandwiched with hot pressing	Room temperature	Activated carbon (Black Pearls 2000)	9.6 Fg^{-1} (at 5 mA/cm^2)	49
Nafion-1100[b]	3.1×10^{-2}	Free-standing film	Sandwiched with hot pressing	Room temperature	Activated carbon (Black Pearls 2000)	13.2 Fg^{-1} (at 5 mA/cm^2)	49
Nafion-115[a]	8.3×10^{-3}	Free-standing film	-	Room temperature	-	-	58
Nafion-115[a]	6×10^{-2}	Free-standing film	Sandwiched with hot pressing	Room temperature	Activated carbon (Norit SA Super or Norit A Supra Eur)	90-130 Fg^{-1} (at 10 mVs^{-1})	51
Nafion-115[a]	-	Free-standing film	Bipolar sandwiched with hot pressing	Room temperature	Activated carbon (Norit A Supra Eur)	114 Fg^{-1} (at 5mHz)	52
Nafion-115[a]	1×10^{-2} (from [54])	Free-standing film	Sandwiched with hot pressing	Room temperature	Carbon (Vulcan XC 72)	20 Fg^{-1} (at 1 mVs^{-1})	53
Nafion[c]/PTFE	1×10^{-3}	Free-standing film	Sandwiched with hot pressing	Room temperature	Carbon (Vulcan XC 72)	16 Fg^{-1} (at 1 mVs^{-1})	54
PFSE/PTFE copolymer[d]	-	Free-standing film	Sandwiched with hot pressing	-	Carbon/graphite fibers	25.2-26.3 Fg^{-1} (at 5 mVs^{-1})	59

Polymer electrolyte	Proton conductivity (Scm^{-1})	Electrolyte production method	Cell design	Testing/storage environment	Electrode active material	Cell capacitance	Ref.
Nafion	-	Solution casting on electrodes	Sandwiched with hot pressing	Room temperature	Graphene	62.3 Fg^{-1} (at 1 Ag^{-1})	55
Nafion	-	Solution casting on electrodes	Sandwiched with hot pressing	Room temperature	Nafion-functionalized reduced graphene oxide	118.5 Fg^{-1} (at 1 Ag^{-1})	55
Nafion[a]	-	Free-standing film	Sandwiched	Room temperature	MWCNTs	57 Fg^{-1} (at 2 mVs^{-1})	56
Nafion[a]	-	Free-standing film	Sandwiched	Room temperature	MWCNTs/ Nafion hybrid	145 Fg^{-1} (at 2 mVs^{-1})	56
Nafion-115[b]	-	Solution casting on electrodes	Sandwiched with pressing	Room temperature, dehydrated film	Aligned CNT/ Nafion hybrid	5-10 Fg^{-1} (at 5 mA)	57
Nafion-115[b]	-	Solution casting on electrodes	Sandwiched with pressing	Room temperature, soaked in 1 M H_2SO_4	Aligned CNT/ Nafion hybrid	28 Fg^{-1} (at 5 mA)	57

[a] Commercial membrane
[b] Re-casted electrolyte film
[c] 5 wt% Nafion solution (equivalent weight=1000)
[d] In solution form (equivalent weight = 900)

3.1.2 Pseudo-capacitors

One of the advantages of PFSA is its compatibility with many pseudocapacitive electrodes that require protons for their redox reactions. The first Nafion-based solid pseudo-capacitor was demonstrated in 1990 by Sarangapani using RuO_2-Nafion composite electrodes.[60] Multi-cell devices based on this configuration demonstrated a capacitance of 0.78 Fcm^{-2} for 3-cell modules and 0.84 Fcm^{-2} for 5-cell modules.[61] In these devices, the Nafion ionomer acts not only as electrolyte but also coats the individual RuO_2 particles and provides continuous proton transport throughout the composite structure. The loading of Nafion ionomers in the RuO_2-Nafion/Nafion/RuO_2-Nafion system was further optimized by Park *et al.*, reaching a cell capacitance of 200 Fg^{-1} with a lifetime of 10,000 cycles.[62] The performance of hydrous RuO_2-Nafion supercapacitors has been characterized at -40 °C for low temperature applications.[63] The highly conductive nature of the electrolyte was mainly attributed to the immersion in liquid H_2SO_4. Other Nafion-based solid pseudo-capacitors were demonstrated using conducting polymer electrodes, including polypyrrole (PPy)/poly(styrene-4-sulphonate) (PSS),[64] and PPy doped with 10-molybdo-2-vanadophosphoric acid or 12-molybdosilicic acid.[65]

Nafion-enabled solid asymmetric supercapacitors demonstrated a potential to further improve energy density when compared to EDLCs while maintaining high rate capability. A hybrid Nafion-enabled supercapacitor in an asymmetric cell configuration with RuO_2/carbon as the positive electrode and carbon as the negative electrode was studied by Staiti *et al*.[59] They showed that optimal performance is obtained by balancing the electrode capacitance in the solid device. An asymmetric Nafion-based supercapacitor

using MnO_2 as positive electrode and carbon as negative electrode delivered a cell capacitance of 48 Fg^{-1}.[66] Although Na^+ was the mobile ion after the cation exchange, the polymer electrolyte showed similar capacitive performance as the liquid electrolyte. A stack of two asymmetric cells separated by two Nafion membranes showed a cell capacitance of 240 Fg^{-1} using polyaniline (PANI)/MWCNT and TiO_2/MWNTs electrodes.[67]

3.1.3 Further improvements

While many PFSA-based solid supercapacitors have been constructed and characterized, few have been developed for commercial supercapacitors. Part of the problem lies in their high cost and sensitivity to dehydration. While PFSA film is highly conductive in a highly hydrated environment at higher temperatures, its proton conductivity drops significantly under ambient conditions. Modification to Nafion through dispersing nanoparticles is a popular approach to improve water retention capability or conductivity. Effects of different hygroscopic materials, such as inorganic oxides particles,[68-72] clays,[58, 73, 74] conductive polymers,[75-77] and solid acids[71, 78] were investigated. However these modified Nafion materials have not been widely tested as polymer electrolytes for supercapacitors and require further study to understand the influence of these modifications on cell capacitance, cycle life, and power performance.

Table 3 Summary of PFSA solid pseudo-capacitors reported in the literature.

Polymer electrolyte	Proton conductivity (Scm^{-1})	Electrolyte production method	Cell design	Testing/storage environment	Electrode active material	Cell capacitance	Ref.
Nafion-117[a]	-	Free-standing film	3-electrode system	-	RuO_2-Nafion	0.6 Fcm^{-2} †	60
Nafion-117[a]	-	Free-standing film	Sandwiched with hot pressing	-	RuO_2-Nafion	0.78 Fcm^{-2} (3-cell)	61
Dow XUS[a]	-	Free-standing film	Sandwiched with hot pressing	-	RuO_2-Dow	0.84 Fcm^{-2} (5-cell)	61
Nafion	-	Free-standing film	Sandwiched with hot pressing	-	RuO_2-Nafion	200 Fg^{-1} (at 20 mVs^{-1})	62
Nafion-115	-	Free-standing film	Sandwiched	soaked in 1 M or 5M H_2SO_4	hydrous RuO_2	165 Fg^{-1} (at 20 mVs^{-1})	63
Nafion-112	-	Free-standing film	Sandwiched	soaked in 1 M or 5M H_2SO_4	hydrous RuO_2	157 Fg^{-1} (at 20 mVs^{-1})	63
Nafion NRE-211	-	Free-standing film	Sandwiched	soaked in 1 M or 5M H_2SO_4	hydrous RuO_2	161 Fg^{-1} (at 20 mVs^{-1})	63
Nafion-117[a]	3×10^{-3}	Solution casting on electrodes	Sandwiched with hot pressing	Stored wet over water	PPy/PSS	20 Fg^{-1} (at 50 mVs^{-1})	64
Nafion-115[a]	-	Free-standing film	3-electrode system	Stored wet over water	PPy doped with 10-molybdo-2-vanadophosphoric acid	7 Fg^{-1} (at 1 mA)†	65

Polymer electrolyte	Proton conductivity (Scm^{-1})	Electrolyte production method	Cell design	Testing/storage environment	Electrode active material	Cell capacitance	Ref.
Nafion-115[a]	-	Free-standing film	3-electrode system	Stored wet over water	PPy doped with 12-molybdosilicic acid	33.4 Fg^{-1} (at 1 mA)[†]	65
PFSE/PTFE copolymer[b]	-	Free-standing film	Asymmetric sandwiched with hot pressing	-	Positive: $RuO_x \cdot nH_2O$/carbon Negative: Carbon	39.5 Fg^{-1} (at 5 mVs^{-1})	59
Nafion-115 in Na^+ form	-	Free-standing film	Sandwiched	Exchanged for 18 h in 0.1M Na_2SO_4	Positive: MnO_2 Negative: Carbon	48 Fg^{-1} (at 5mA)	66
Nafion	-	Free-standing film	Bipolar sandwiched with hot pressing	-	PANI/MWCNT and TiO_2/MWNTs	240 Fg^{-1} (2-cell)	67

[a] Commercial membrane
[b] In solution form (equivalent weight = 900)
[†] Single electrode capacitance

3.2 Sulfonated hydrocarbon electrolytes

Nafion is rather costly and the preparation of Nafion involves environmentally unfriendly fluorine-based technologies.[47, 48] Non-perfluorinated alternatives based on hydrocarbon backbones have been developed (see Tables 4 and 5). Most of them are composed of benzene rings or aromatic heterocyclic rings. The wide variability of their chemical structures permits different functionalization (i.e. introduction of polar sites) through doping, chemical grafting, or direct sulfonation to increase proton conductivity and water uptake. Some of these alternative sulfonated hydrocarbon-based proton conductors include poly(ether sulfones) (PES) and poly(ether ketones) (PEK) with varying numbers of ether and ketone functionalities (such as poly(ether ether ketone) (PEEK), poly(ether ether ketone ketone) (PEEKK), poly(arylen ethers), polyesters, or polyimides). These materials have excellent chemical resistance due to the higher C-H bond strength in the benzene ring compared with aliphatic C-H bond strengths. Other advantages of these materials include lower cost, excellent chemical resistance, and good mechanical properties.

Although numerous acid-functionalized hydrocarbon proton conductors have been prepared, their overall performance is still inferior to Nafion. Currently, most efforts on sulfonated hydrocarbon proton conductors are focused on fuel cell applications, especially for proton exchange membrane fuel cells or direct methanol fuel cells, due to their higher temperature stability and lower fuel cross-over. Application of this group of materials to supercapacitors is limited. An overview of the proton conductivity of sulfonated poly(ether ether ketone) (SPEEK) and sulfonated poly (ether ether ketone ketone) (SPEEKK) at different degrees of sulfonation as well as blends with

polybenzimidazole (PBI) or PES and pure oligomers is shown in Fig. 6. Due to their higher proton conductivity at low temperatures, this section focuses on the application of SPEEKK and SPEEK (or other PEK with different ether and ketone functionalities) for supercapacitor applications.

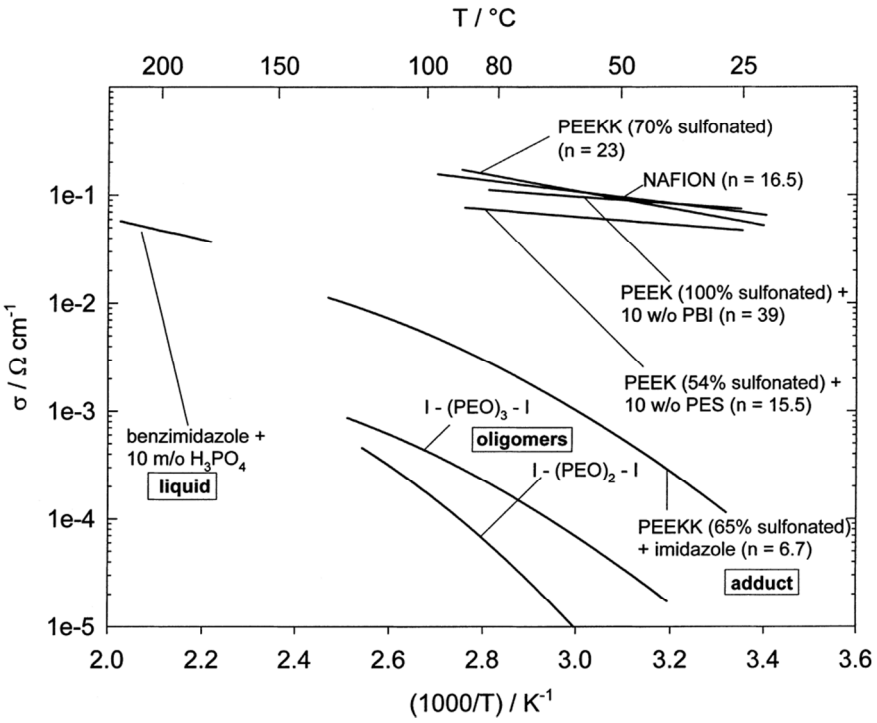

Fig. 6 Comparison of proton conductivity of various fully hydrated sulfonated polymer electrolytes, including liquids, adducts, and oligomers containing heterocycles as proton solvent. Reprinted with permission from Kreuer.[79] Copyright 2001 Elsevier.

3.2.1 Electrochemical double layer capacitors

The first solid EDLC based on SPEEK membranes was demonstrated by Kim *et al.* in 2006.[80] The SPEEK film was obtained by sulfonation of commercial PEEK followed by solution casting and soaking in H_2SO_4. The free-standing film exhibited a conductivity of 4.3×10^{-3} Scm^{-1} at room temperature. After 1,000 cycles, the solid EDLC showed a 5% reduction in capacitance to 131 Fg^{-1}. Further studies were conducted with differing degrees of sulfonation to improve cell performance.[81] The polymer electrolytes

showed a maximum conductivity of 4.5×10^{-3} Scm^{-1} at 78% sulfonation. Since a higher degree of sulfonation may further restrict mass transport due to the interactions among the polar -SO_3H groups while a lower degree of sulfonation may impose higher resistance, an optimization of sulfonation is essential to achieve good EDLC cell performance.

In addition to SPEEK, sulfonated poly(fluorenyl ether nitrile oxynaphthalate) (PFENO) co-polymers at different degrees of sulfonation have been investigated to improve dimensional stability and promote better electrode/polymer electrolyte adhesion.[82] Similar to SPEEK membranes, H_2SO_4 was well encapsulated in the polymer membrane after soaking. Optimized EDLC performance was achieved at 40% sulfonation. Poly(styrenesulfonic acid) film has also been investigated as polymer electrolyte for CNT EDLCs.[83] The properties of the polymer electrolyte and the performance of the devices were characterized as a function of RH. The cell capacitance increased with RH, reaching 85 Fg^{-1}. Poly(styrenesulfonic acid) exhibits a lower conductivity of 1.5×10^{-3} Scm^{-1}, even at 80% RH, when compared to SPEEK films.

In order to improve the conductivity of SPEEK, $LiClO_4$ was added into the dissolved SPEEK solution.[84] Ionic conductivity increased with increasing $LiClO_4$ content. A maximum conductivity of 1.1×10^{-2} Scm^{-1} was achieved with 9.5 wt.% $LiClO_4$. Since no soaking in aqueous H_2SO_4 or water was performed for these polymer electrolytes, lithiated SPEEK contained limited water content. The enabled solid EDLCs with activated carbon electrodes could be cycled from 0 V to 1.8 V without significant polarization at high voltages and showed a high capacitance of 190 Fg^{-1}. However, the contributions of H^+ and Li^+ ions to the ionic conductivity of the lithiated SPEEK polymer electrolyte are not known and further characterizations are required.

Table 4 Summary of sulfonated hydrocarbon solid EDLCs reported in the literature.

Polymer electrolyte	Degree of sulfonation	Proton conductivity (Scm^{-1})	Electrolyte production method	Cell design	Testing/storage environment	Electrode active material	Cell capacitance	Ref.
Sulfonated commercial PEEK	67%	4.3×10^{-3}	Free-standing film	Sandwiched and vacuum-sealed	Soaked in 0.25 M H_2SO_4 before cell assembly	Activated carbon (MSC 30)	138.4 Fg^{-1} (at 2 $mAcm^{-2}$)	80
Sulfonated commercial PEEK	58%-83%	4.5×10^{-3} (at 78% sulfonation)	Free-standing film	Sandwiched and vacuum-sealed	Soaked in 0.25 M H_2SO_4 before cell assembly	Activated carbon (MSC-30)	161 Fg^{-1} (70% sulfonation at 5 $mAcm^{-2}$)	81
Sulfonated PFENO copolymer	21%-51%	6×10^{-3} (at 51% sulfonation)	Free-standing film	Sandwiched and vacuum-sealed	Soaked in 0.5 M H_2SO_4 before cell assembly	Activated carbon (MSC-30)	158 Fg^{-1} (40% sulfonation at 20 $mAcm^{-2}$)	82
Poly(styrene-sulfonic acid)	-	1.5×10^{-3} (at 80% RH)	Free-standing film	Sandwiched with hot pressing	RH controlled environment	CNT	85 Fg^{-1} (at 80% RH, 1 $mAcm^{-2}$)	83
Lithiated and sulphonated PEEK[a]	65%	1.1×10^{-2} (with 9.5 wt.% $LiClO_4$)	Solution casting on electrodes	Sandwiched	-	Activated carbon (TF-B520)	190 Fg^{-1} (with 9.5 wt.% $LiClO_4$, at 50 $mVs^{-1)}$	84

[a] Casted film

3.2.2 Pseudo-capacitors

SPEEK has also been used as proton-conducting polymer electrolyte for solid pseudo-capacitors. For example, Sivaraman *et al.* demonstrated a solid supercapacitor with PANI as electrode material.[85] The relatively low capacitance of 28 Fg^{-1} of this device was due to the solvent effect resulting from the electrolyte casting and electrode preparation procedures, where dimethyl formamide (DMF) and dimethyl acetamide (DMAC) may have led to the formation of dimethyl amine (DMA) and reacted with the sulfonic groups in SPEEK, thus reducing the proton conductivity of the electrolyte. A water/isopropyl alcohol mixture was selected as an alternative solvent to prepare SPEEK membranes with a controlled amount of cross-linking.[86] A sandwiched 6-cell stack solid supercapacitor based on the cross-linked SPEEK polymer electrolyte and a PANI electrode achieved a specific capacitance of 480 Fg^{-1}.[87]

Other sulfonated hydrocarbon-based polymer electrolytes have been explored for solid pseudo-capacitors. For example, a pseudo-capacitor with composite PANI electrodes and a poly(vinyl sulfonic acid) proton-conducting polymer electrolyte optimized for fast ion transport and intimate electrode/electrolyte contact demonstrated a good capacitance of 98 Fg^{-1}.[88] However, the solid device exhibited an approximately 20% reduction in capacitance after 1,500 cycles due to the degradation of both the electrolyte and the PANI electrodes.

3.2.3 Further improvements

Sulfonated hydrocarbon polymers offer a more convenient and less expensive process than those used to fabricate PFSA membranes. As the backbones of these sulfonated polymers tend to be less hydrophobic and the acid groups are less polar, a high

degree of hydration is required to maintain a sufficient level of proton conductivity at room temperature. For instance, water filled channels in SPEEK are narrower than those in Nafion, leading to a larger hydrophilic/hydrophobic interface and a larger separation of neighboring sulfonic acid functional groups.[79] In order to achieve better and stable supercapacitor device performance, enhancements in proton conductivity of PFSA films and sulfonated hydrocarbons at low RH conditions are required. Nevertheless, due to their higher temperature stability, sulfonated hydrocarbon proton conductors (especially those containing aromatic backbones) are attractive alternatives for high temperature supercapacitor applications.[89-91]

Table 5 Summary of sulfonated hydrocarbon pseudo-capacitors reported in the literature.

Polymer electrolyte	Degree of sulfonation	Proton conductivity (Scm^{-1})	Electrolyte production method	Cell design	Testing/storage environment	Electrode active material	Cell capacitance	Ref.
Sulfonated commercial PEEK[a]	65%	-	Free-standing film	Sandwiched with hot pressing	Room temperature	Polyaniline/ Carbon/ SPEEK	27 Fg^{-1} (at 5 mVs^{-1})	85
Cross-linked SPEEK[a]	65%	1.2×10^{-2}	Free-standing film	Sandwiched with hot pressing	-	Polyaniline/ Carbon	480 Fg^{-1} (at 2 $mAcm^{-2}$)[†]	86
Cross-linked SPEEK[a]	65%	-	Free-standing film	Bipolar sandwiched with hot pressing	Room temperature	Polyaniline/ Carbon	480 Fg^{-1} (at 10^{-2} Hz)[†]	87
Polyvinyl sulfonic acid	-	-	Free-standing film	Sandwiched with hot pressing	-	Polyaniline/ Carbon	98 Fg^{-1} (at 10 mVs^{-1})	88

[a] Casted film
[†] Weight of PANI materials of single electrode

4 Inorganic/polymer proton-conducting electrolytes and enabled supercapacitors

Inorganic/polymer proton-conducting electrolytes can be further divided into two subgroups: (a) salt-in-polymer and (b) polymer-in-salt. Salt-in-polymer electrolytes are prepared by dispersing acids, bases, or salts in a polymer such as PEO, poly(acrylonitrile) (PAN), or poly(methylmethacrylate) (PMMA). Most salt-in-polymer electrolytes are aqueous based and form acid/polymer blends or acidic hydrogels (i.e. aqueous gels). In contrast, polymer-in-salt electrolytes are prepared by using only a small amount of polymer material as a matrix to hold the solid proton conductors together during film forming. With increasing salt concentration, the discrete salt clusters are interconnected, forming a percolation pathway for ion conduction. Although the ionic conductivity of such electrolytes is 100 to 1000 times less than that of liquid electrolytes, this is less problematic as a thin film supercapacitor (due to the reduced electrolyte thickness) can largely compensate for the reduction in ionic conductivity. Since many highly conductive proton-conductors rely on the water molecules embedded in the structure (e.g. crystallized water in hydrous acids) to conduct the protons rather than on the loosely bound or free water, polymer-in-salt electrolytes have much higher water retention capability compared to salt-in-polymer electrolytes.

4.1 Acid/polymer blend electrolytes

Acid/polymer blends result from mixing strong acids (e.g. H_2SO_4 or H_3PO_4) with polymers and are currently the most widely used polymer electrolytes for supercapacitors, especially for flexible and micro-devices. Unlike polymeric proton-conducting

electrolytes (discussed in Section 3), which have been deployed primarily for rigid solid supercapacitors, acid/polymer blends have found a wide-range of applications in flexible solid devices due to their ease of preparation, good conductivity, and high environmental stability. In addition to avoiding electrolyte leakage, acid/polymer blend electrolytes can reduce device thickness and packaging. Polymers used in such systems include PEO, PVA, PAAM, poly(vinylpyrrolidone) (PVP), poly(2-vinylpyridine) (P_2VP), and poly(4-vinylpyridine) (P_4VP). H_2SO_4 and H_3PO_4 are often chosen as proton conductors due to their self-ionization and self-dehydration reactions[27] at pure states:

$$6H_2SO_4 \leftrightarrow H_3SO_4^+ + H_3O^+ + HSO_4^- + HS_2O_7^- + H_2S_2O_7 + H_2O$$

$$5H_3PO_4 \leftrightarrow 2H_4PO_4^+ + H_3O^+ + H_2PO_4^+ + H_2P_2O_7^{2-}$$

Even though polymers are less efficient than water in dissociating protons, the proton conductivity of acid/polymer blends falls between aqueous acidic solutions and pure acids.

Acid/polymer blend electrolytes are prepared by adding an acid solution to an aqueous polymer solution under stirring. This process can be applied only when mixing with aqueous acids does not result in chemical degradation of the polymer. They typically display a room temperature conductivity in the range from 10^{-6} to 10^{-4} Scm^{-1} in the anhydrous state.[27] One of the first systems (H_3PO_4/PVA) for electrochemical applications has been described by Polak *et al.* in 1987.[92]

4.1.1 Electrochemical double layer capacitors

Acid/polymer blend electrolytes, in particular H_2SO_4/PVA, have been widely used for EDLCs with CNT or graphene electrodes, to achieve flexible and solid-state structures (Table 6). PVA is widely used due to its good thin film forming capability,

high water-solubility, and adhesive characteristics which ease processing. For example, Wu *et al.* developed in-plane micro-supercapacitors using graphene electrodes in an H_2SO_4/PVA electrolyte, which showed an areal capacitance of 80.7 μFcm^{-2} and were able to be charged/discharged at a 1,000 Vs^{-1} scan rate.[93] The in-plane cell design minimized the ion diffusion pathways and led to a time constant of 0.28 ms. Figs. 7a and b compare capacitance and impedance of a flexible solid EDLC using H_2SO_4/PVA and 3D graphene hydrogel electrodes to a 1 M H_2SO_4 liquid device.[94] The solid device showed a high areal capacitance of 372 $mFcm^{-2}$ (or 186 Fg^{-1}) and slightly larger ESR, lower leakage current, and less capacitance decay after 10,000 cycles than the liquid device. H_2SO_4/PVA polymer electrolytes have also been combined with other advanced electrode materials, such as cellulose nanofibers/MWCNTs hybrid aerogel[95] or CNT coated cellulose paper[96], to fabricate solid-state flexible EDLCs.

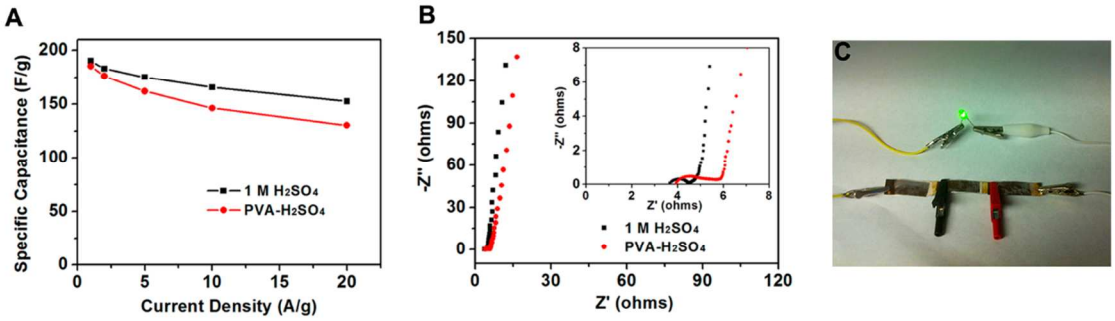

Fig. 7 Comparison of EDLC cells with H_2SO_4/PVA gel electrolyte and a 1M H_2SO_4 solution: (a) specific capacitances as a function of current density; (b) impedance response in Nyquist plots (inset shows the magnified high-frequency region); and (c) photograph of a green LED powered by three supercapacitors in series. Reprinted with permission from Xu *et al.*[94] Copyright 2013 American Chemical Society.

The addition of a redox active mediator into the polymer electrolyte may further enhance cell performance. Senthilkumar *et al.* added sodium molybdate (Na_2MoO_4) into an H_2SO_4/PVA blend system and found increased capacitance and energy density.[97] An activated carbon based EDLC demonstrated a 57.2% increase in specific capacitance

after introducing Na_2MoO_4 (Fig. 8), due to the reaction between Mo(VI)/Mo(V) and Mo(VI)/Mo(IV) redox couples. However, the addition of the mediator may limit the rate performance of the solid device, depending on the reaction kinetics. Another redox mediator used in H_2SO_4/PVA is p-benzenediol.[98] In addition to the double layer capacitance provided by activated carbon, p-benzenediol/p-benzoquinone redox couples in the electrolyte contributed Faradaic pseudo-capacitance. However, this reaction occurred only from -0.5 to 0.5 V, thus its contribution to the total cell capacitance in the desired potential range (0 to 1 V and higher) is limited. In addition, leakage current and self-discharge need to be characterized for electrolytes with such mediators.

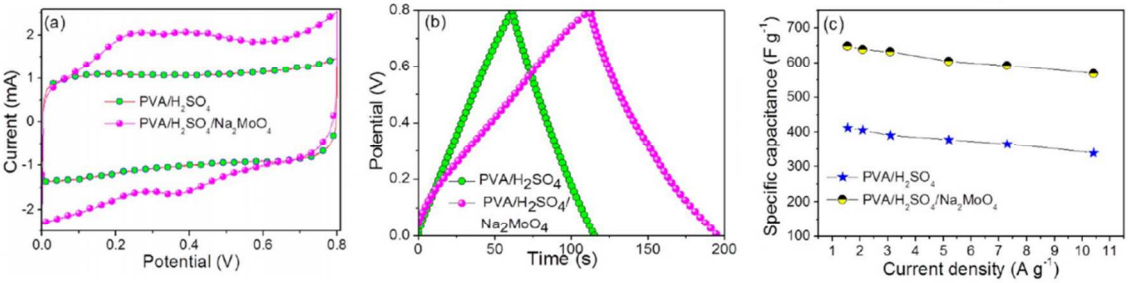

Fig. 8 Comparison of supercapacitor cells with and without Na_2MoO_4 in H_2SO_4/PVA gel electrolyte: (a) CV curves at 10 mVs^{-1}, (b) charge/discharge curves at 1.56 Ag^{-1}, and (c) specific capacitance as a function of current density. Reprinted with permission from Senthilkumar *et al.*[97] Copyright 2013 American Chemical Society.

H_3PO_4/PVA is another common acid/polymer blend system for flexible devices. Kaempgen *et al.* used H_3PO_4/PVA with single-wall carbon nanotube (SWCNT) electrodes to construct printable thin film EDLCs that showed lower internal resistance and higher capacitance than a liquid device.[99] An in-plane EDLC comprised of pristine graphene or multilayer reduced graphene oxide electrodes and a H_3PO_4/PVA polymer electrolyte was fabricated as a 2D solid device.[100] Due to the high internal resistance, the device showed poor performance at high charge/discharge rates.

El-Kady *et al.* demonstrated a high rate flexible EDLC, consisting of an H_3PO_4/PVA polymer electrolyte and graphene electrodes.[101] The electrodes were obtained by direct laser reduction of graphite oxide films so that the resultant film allowed the elimination of binders and current collectors. The capacitance of the solid device was comparable to the capacitance obtained from an aqueous electrolyte (Fig. 9). The shelf life and cycle life of the device were tested over a 4-month storage period and 10,000 cycles and indicated excellent stability without performance degradation.

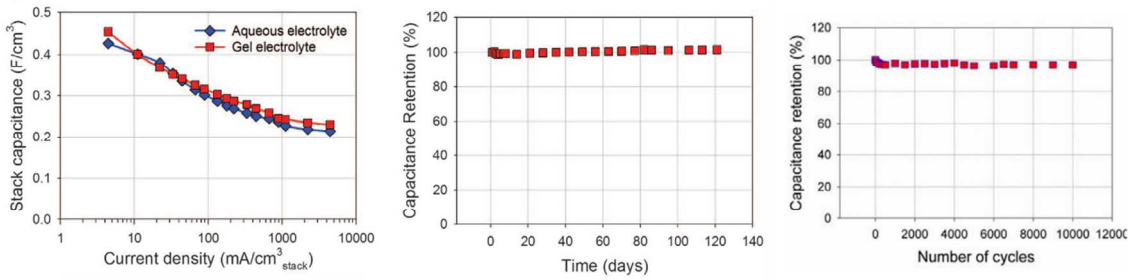

Fig. 9 (a) Comparison of supercapacitor performance using gelled versus aqueous electrolytes in terms of specific capacitance as a function of current density. (b) A shelf-life test shows excellent stability of the solid cell for over 4 months. (c) Cycling stability of the solid capacitor. Reprinted with permission from El-Kady *et al.*[101] Copyright 2012 AAAS.

Chen *et al.* demonstrated a coaxial fiber-type flexible EDLC with an H_3PO_4/PVA polymer electrolyte between aligned CNT fibers.[102] The highly aligned CNT showed high mechanical strength, and could be woven into a textile structure for flexible or wearable electronics. Nevertheless, the device showed high internal resistance.

PEO-modified polymethacrylate (PMA) dissolving anhydrous H_3PO_4 has been investigated as a polymer electrolyte for solid EDLCs.[103] A maximum conductivity of 2.1×10^{-4} Scm^{-1} was achieved with optimized amounts of organic plasticizers (poly(ethylene glycol) dimethylether) at room temperature. Utilizing activated carbon electrodes, the solid device showed similar capacitance as an aqueous device. Since good rate performance could only be achieved at a high temperature of 90 °C, further

improvement in low to room temperature conductivity is necessary for practical supercapacitor applications.

Table 6 Summary of acid/polymer blend EDLCs reported in the literature.

Electrolyte blend	Acid concentration*	Electrolyte production method	Cell design	Electrode active material	Cell capacitance	Time constant (ms)	Ref.
H_2SO_4/PVA	-	Solution casting on electrodes	Interdigitated finger	Reduced graphene film	80.7 μFcm^{-2} (at 10^{-2} Hz)	0.28	93
H_2SO_4/PVA	50 wt.%	Solution casting on electrodes	Sandwiched with pressing	Graphene hydrogel	372 $mFcm^{-2}$ (at 1 Ag^{-1})	-	94
H_2SO_4/PVA	50 wt.%	Electrodes soaked in polymer electrolyte solution	Sandwiched with pressing	Cellulose nanofibers/ MWCNTs	178 Fg^{-1} (at 5 mVs^{-2})	-	95
H_2SO_4/PVA	ca. 50 wt.%	Electrodes soaked in polymer electrolyte solution	Sandwiched with pressing	CNTs	273 Fg^{-1} (at 10 mA)	-	96
H_2SO_4/PVA/ Na_2MoO_4	-	Solution casting on electrodes	Sandwiched	Activated carbon	648 Fg^{-1} (at 1 Ag^{-1})	500	97
H_2SO_4/PVA/ P-benzenediol	-	Free-standing film	Sandwiched	Activated carbon	474 Fg^{-1} (from -0.5 V to 0.5 V at 1 Ag^{-1})	-	98
H_3PO_4/PVA	44 wt.%	-	Sandwiched	SWCNTs	110 Fg^{-1} (at 1 mAg^{-1})	-	99
H_3PO_4/PVA	44 wt.%	Solution casting on electrodes	Interdigitated finger	Graphene	40 μFcm^{-2} (at 630 $mAcm^{-2}$)	-	100
H_3PO_4/PVA	44 wt.%	Solution casting on electrodes	Interdigitated finger	Multilayer reduced graphene oxide	197 μFcm^{-2} (at 281 $nAcm^{-2}$)	-	100
H_3PO_4/PVA	40 wt. %	Solution casting on electrodes	Sandwiched	Reduced graphite oxide	0.4 $mFcm^{-3}$ (at 10 $mAcm^{-3}$)	-	101
H_3PO_4/PVA	46 wt.%	Electrodes soaked in polymer electrolyte solution	Coaxial fiber	Aligned CNT fiber and sheet	8.66 $mFcm^{-2}$	-	102

Electrolyte blend	Acid concentration*	Electrolyte production method	Cell design	Electrode active material	Cell capacitance	Time constant (ms)	Ref.
H_3PO_4/PEO-PMA	-	Free-standing film	Sandwiched	Activated carbon fiber	120 Fg^{-1} (at 0.5 $mAcm^{-2}$)	-	103

* Calculated based on pure acid/polymer weight

4.1.2 Pseudo-capacitors

Acid/polymer blend electrolytes are commonly used in pseudo-capacitive systems such as RuO_2, MnO_2, and conducting polymers (Table 7). For example, nano-crystalline RuO_2 thin films were deposited on a stainless steel mesh by chemical deposition at different temperatures.[104] The resultant RuO_2 thin films were solidified in and separated by the H_2SO_4/PVA polymer electrolyte. At room temperature this device exhibited a capacitance of 234 Fg^{-1} and an ESR of 0.63 Ω. The rate performance of this solid device was limited by its high charge transfer resistance of 10.95 Ω. Si *et al.* demonstrated an on-chip micro-supercapacitor, based on MnO_x/Au multilayers electrodes leveraging an H_2SO_4/PVA polymer electrolyte, and compared it to a bare MnO_x device.[105] The surface adsorption/desorption of protons and the rapid and highly reversible redox reaction between MnO_x and protons enabled high rate performance. The low frequency capacitance for the MnO_x/Au device reached 60 Fcm^{-3} with a 5.9 ms time constant. However, this device displayed a nearly 25% eduction in capacitance after 15,000 cycles, probably due to the electrochemical dissolution of active materials. Other H_2SO_4/PVA-enabled pseudo-capacitors, including nano-$GeSe_2$[106] and nitrogen and boron co-doped graphene[107] have been demonstrated.

H_2SO_4/PVA polymer electrolytes have also been applied to PANI-based solid pseudo-capacitors. A thin solid pseudo-capacitor was demonstrated using two slightly separated PANI-based electrodes solidified in the electrolyte.[108] The solid and liquid device exhibited a similar CV curve and similar capacitance (332 Fg^{-1} *vs.* 360 Fg^{-1}, respectively). Other H_2SO_4/PVA enabled pseudo-capacitors with PANI electrodes have been demonstrated, including PANI coated graphitic petals on carbon cloth[109] and PANI

coated carbon paper.[110] Leveraging micro-fabrication and in-situ chemical polymerization methods, on-chip micro-supercapacitors have been demonstrated with patterned PANI electrodes.[111, 112]

H_3PO_4/PVA is also often selected as polymer electrolyte for solid pseudo-capacitors. The first H_3PO_4/PVA-based pseudo-capacitor was developed as a solid multi-cell RuO_2 device in single cell, 4-cell, and 9-cell configurations.[113] The solid device could be charged and discharged at a scan rate of 10 Vs^{-1}. An interdigitated MnO_2-based pseudo-capacitor with an H_3PO_4-PVA semi-dried gel acting as both electrolyte and substrate was developed.[114] MnO_2 nanoparticle electrode fingers were prepared by microfluidic etching. While the device had stable cycle life, it showed a distorted CV at a 100 mVs^{-1} scan rate. H_3PO_4/PVA electrolytes have also been utilized for pseudo-capacitors with MnO_2 composite electrodes, such as MnO_2/carbon core-shell fiber,[115] MnO_2/carbon nanoparticles,[116] MnO_2/graphene nanosheets,[117] and MnO_2/PPy.[118] In particular, the MnO_2/carbon core-shell fiber solid capacitor showed high rate capability with a scan rate of up to 20 Vs^{-1} and a volumetric capacitance of 2.5 Fcm^{-3}.

H_3PO_4/PVA electrolytes have also been applied to PANI-based pseudo-capacitors. Xue *et al.* developed an H_3PO_4/PVA-based solid micro-pseudo-capacitor with PANI nanorod electrodes.[119] The highly ordered vertical nanorod arrays were prepared by electrodeposition of PANI on flat reduced graphene oxide patterns. The H_3PO_4/PVA electrolyte was coated on the interdigitated finger electrodes as well as the current collector. A similar flexible device was developed by growing PANI on Au coated printing paper.[120] The synthesized PANI fibers were found to be twisted and tangled with each other, forming uniform and porous networks. The polymer electrolyte solution

penetrated into the framework before solidification, facilitating proton transport between PANI and the electrolyte, and enabled a consistent areal capacitance of ca. 50 $mFcm^{-2}$ under a discharge current increasing from 0.1 to 2 $mAcm^{-2}$. In addition, flexible pseudo-capacitors based on nano-composite electrodes consisting of PANI and CNT, SiO_2, TiO_2, or graphene flakes were characterized.[121] A stack of 8 flexible supercapacitor cells was demonstrated using a sandwiched cell configuration enabled by an H_3PO_4/PVA electrolyte.

4.1.3 Further improvements

The rate performance of current flexible EDLCs and pseudo-capacitors is mainly limited by the kinetics of ion adsorption/desorption at the electrode/electrolyte interface and/or the kinetics of pseudo-capacitive reactions (i.e. charge transfer reactions), rather than the movement of ionic species in the polymer electrolyte. Although both H_3PO_4/PVA and H_2SO_4/PVA have been shown as suitable polymer electrolytes with good stability, the low proton conductivity of these systems limit the rate performance of the enabled solid devices. In order to enhance the proton conductivity of the acid/polymer blend electrolytes, polymers with intermediate basicity could be used, such as PAAM and PVP. In such cases, the nitrogen or oxygen atoms in the polymer can be protonated by the acid, leading to additional proton exchange and conduction. For example, a proton conductivity of 6×10^{-3} Scm^{-1} was observed for an H_2SO_4/PAAM blend.[34] However very limited electrochemical studies investigating their compatibility with supercapacitor devices have been performed on such systems.

Table 7 Summary of acid/polymer blend electrolyte-based pseudo-capacitors reported in the literature.

Electrolyte blend	Acid concentration*	Electrolyte production method	Cell design	Electrode active material	Cell capacitance	Time constant (ms)	Ref.
H_2SO_4/PVA	-	Electrodes soaked in polymer electrolyte solution	Sandwiched with pressing	RuO_2 thin film	234 Fg^{-1} (at 5 mVs^{-1})	-	104
H_2SO_4/PVA	65 wt.%	Solution casting on electrodes	Interdigitated finger	MnO_x	41.4 Fcm^{-3} (at 10 mHz)	5.9	105
H_2SO_4/PVA	65 wt.%	Solution casting on electrodes	Interdigitated finger	MnO_x/Au	58.3 Fcm^{-3} (at 10 mHz)	4.7	105
H_2SO_4/PVA	50 wt.%	Electrodes soaked in polymer electrolyte solution	Sandwiched with pressing	$GeSe_2$	186 µF (at 100 mAm^{-2})	-	106
H_2SO_4/PVA	50 wt.%	Electrodes soaked in polymer electrolyte solution	Interdigitated finger	$GeSe_2$	200 µF (at 100 mAm^{-2})	-	106
H_2SO_4/PVA	50 wt.%	Electrodes soaked in polymer electrolyte solution	Sandwiched with pressing	nitrogen and boron co-doped graphene	62 Fg^{-1} (at 5 mVs^{-1})	-	107
H_2SO_4/PVA	50 wt.%	Electrodes soaked in polymer electrolyte solution	Sandwiched with pressing	PANI on CNT	332 Fg^{-1} (at 1 Ag^{-1})	-	108
H_2SO_4/PVA	50 wt.%	Electrodes soaked in polymer electrolyte solution	Sandwiched	PANI coated graphitic petals	1.5 Fcm^{-2} (at 1 Ag^{-1})	-	109
H_2SO_4/PVA	50 wt.%	Solution casting on electrodes	Sandwiched with pressing	PANI coated carbon paper	1 Fcm^{-2} (at 0.5 Ag^{-1})	-	110
H_2SO_4/PVA	-	Solution casting on electrodes	Interdigitated finger	PANI on Au/Cr	588 Fcm^{-3} (at 0.1 $mAcm^{-2}$)	-	111

Electrolyte blend	Acid concentration*	Electrolyte production method	Cell design	Electrode active material	Cell capacitance	Time constant (ms)	Ref.
H_2SO_4/PVA	44 wt.%	Solution casting on electrodes	Interdigitated finger	PANI	20.4 $mFcm^{-2}$ (at 0.3 $mAcm^{-2}$)	-	112
H_3PO_4/PVA	40 wt.%	Free-standing film	Interdigitated finger	MnO_2 nanoparticles	338.1 Fg^{-1} (at 0.5 $mAcm^{-2}$)	-	114
H_3PO_4/PVA	46 wt.%	Solution casting on electrodes	Interdigitated finger	MnO_2/carbon core-shell fiber	2.5 Fcm^{-3} (at 20 $mAcm^{-3}$)	22	115
H_3PO_4/PVA	46 wt.%	Electrodes soaked in polymer electrolyte solution	Sandwiched	MnO_2/carbon nanoparticles	800 Fg^{-1} (at 5 mVs^{-1})†	500	116
H_3PO_4/PVA	-	Solution casting on electrodes	Interdigitated finger	MnO_2/graphene nanosheets	267 Fg^{-1} (at 0.2 Ag^{-1})	-	117
H_3PO_4/PVA	46 wt.%	Electrodes soaked in polymer electrolyte solution	Interdigitated finger	PPy/MnO_2	69.3 Fcm^{-3} (at 0.1 Acm^{-3})	16	118
H_3PO_4/PVA	40 wt.%	Solution casting on electrodes	Interdigitated finger	PANI on reduced graphene oxide	970 Fg^{-1} (at 2.5 Ag^{-1})	-	119
H_3PO_4/PVA	46 wt.%	Electrodes soaked in polymer electrolyte solution	Sandwiched	PANI on Au-covered paper	50 $mFcm^{-2}$ (at 0.1 $mAcm^{-2}$)	-	120
H_3PO_4/PVA	-	Free-standing film	Sandwiched	PANI/CNT/TiO_2 on graphite	477.1 Fg-1 (at 0.4 μAmm^{-2})	-	121

* Calculated based on pure acid/polymer weight
† Single electrode capacitance

4.2 Acidic hydrogel electrolytes

In order to increase the proton conductivity of acid/polymer blend electrolytes, gel polymer electrolytes are developed by using low molecular-weight organic solvents, such as ethylene carbonate (EC), propylene carbonate (PC), DMF, or diethyl carbonate (DEC). When water is used as a solvent, the gel polymer electrolyte is referred to as hydrogel (or aqueous gel) polymer electrolyte.

Hydrogel polymer electrolytes utilize superabsorbent or highly swollen polymers, such as poly(vinyl alcohol) (PVA), poly(acrylic acid) (PAA), and poly(acrylamide) (PAAM), or physically or chemically cross-linked polymers as host materials. Due to interactions between the –OH and/or =O groups of the polymer and the acidic solutions, swelling of the polymer occurs throughout the structure by hydrogen bonding. To maintain the water-insolublity of the hydrogel, the polymer hosts are often chemically or physically cross-linked. As shown in Fig. 10, chemically cross-linked polymer monomers are covalently bonded by a chemical cross-linker, whereas the physically cross-linked polymer hosts are non-covalently bonded but the polymer host is stabilized by small polymer domains (typically crystalline domains), and thus exhibit less stability. The three-dimensional networks in the polymer are able to trap acidic solutions in the polymer matrix.

The basic ion conduction principle of hydrogel polymer electrolytes is similar to aqueous electrolytes, in that ionic conduction relies on the excess water that the system contains. Acidic hydrogel electrolytes have been developed using PVA[122] and PAAM[123] with strong acids and can achieve a room temperature proton conductivity as high as 10^{-2} to 10^{-1} Scm^{-1}.

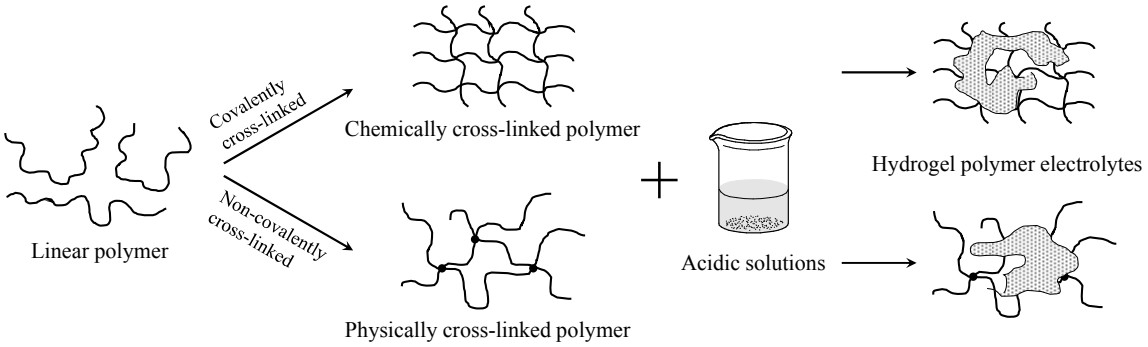

Fig. 10 Schematic of hydrogel polymer electrolyte preparation from chemically or physically cross-linked polymers with acidic solutions.

4.2.1 Electrochemical double layer capacitors

A summary of acid hydrogel-based EDLCs is given in Table 8. PVA is the most commonly used polymer matrix for acidic hydrogels. Wada *et al.* used glutaraldehyde (GA) to cross-link PVA in a PVA-H_2SO_4 hydrogel electrolyte as a free-standing membrane for activated carbon EDLCs.[122] The device showed a capacitance and rate performance similar to a 1 M H_2SO_4 liquid cell, as shown in Fig. 11a. The self-discharge of the hydrogel enabled-EDLC was suppressed by using a hydrogel polymer electrolyte with a smaller leakage current (Fig. 11b).

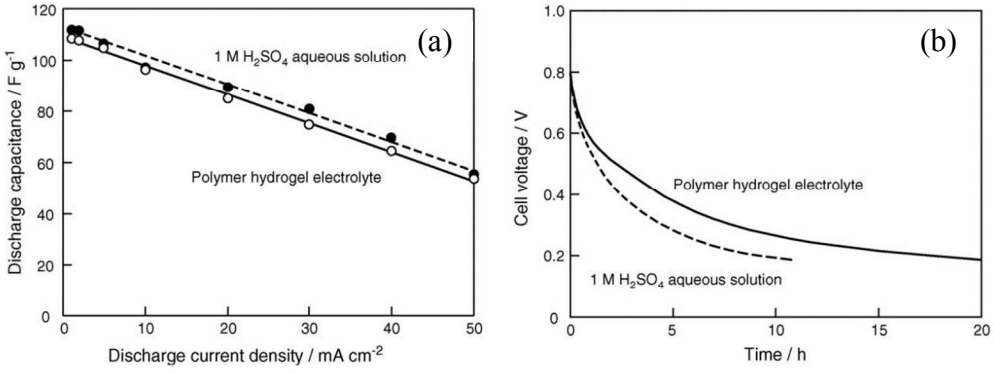

Fig. 11 Comparison of EDLC cells with a polymer hydrogel electrolyte and a 1 M H_2SO_4 aqueous solution: (a) specific capacitance as a function of current density and (b) self-discharge over time. Reprinted with permission from Wada *et al.*[122] Copyright 2006 Elsevier.

A more concentrated 4 M H_2SO_4 solution with GA cross-linked PVA was used to construct activated carbon EDLCs, and showed higher proton conductivity than a film containing 1 M H_2SO_4.[124] The EDLCs exhibited higher capacitance but raise concerns over the chemical stability of hydrogels containing such high concentration of H_2SO_4.

Perchloric acid ($HClO_4$) has also been used as proton donor. Sampath *et al.* prepared GA cross-linked PVA hydrogels with varying $HClO_4$ content.[125] The average conductivity of the resultant polymer electrolyte was in the 10^{-3} Scm^{-1} range. The glass transition temperature of the hydrogels decreased with increasing $HClO_4$ content (from 0.1 M to 2 M), while the capacitance of the enabled black pearl carbon EDLC increased from 12.8 to 91.2 Fg^{-1}. To further improve water retention capacity, film integrity, and mechanical properties of cross-linked PVA hydrogels, a GA cross-linked PVA/PAA-$HClO_4$ blend system was investigated,[126] where the protons in the side chains of PAA could be dissociated to promote higher proton density. With increasing amounts of PAA, the proton conductivity increased from 10^{-3} to 10^{-2} Scm^{-1}, mainly due to enhanced proton hopping. This hydrogel electrolyte followed the VTF relation over temperature with an activation energy of 0.15 eV.

A cellulose/chitin hybrid gel electrolyte containing binary ionic liquids and aqueous 2 M H_2SO_4 has been developed.[127] The activated carbon EDLC based on this hybrid gel electrolyte exhibited even higher capacitance than that of a liquid cell (162 Fg^{-1} vs. 155 Fg^{-1}). It also showed excellent high-rate discharge capability and 80% capacitance retention over 100,000 cycles at 5,000 mAg^{-1}. As another example, a PAAM-based hydrogel with H_2SO_4 in activated carbon[128] enabled an EDLC which showed a

performance similar to a liquid cell (30 wt.%) with the same time constants (Fig. 12). The hydrogel electrolyte was composed of 5 wt.% PAAM, 29 wt.% H_2SO_4, and 66 wt.% H_2O.

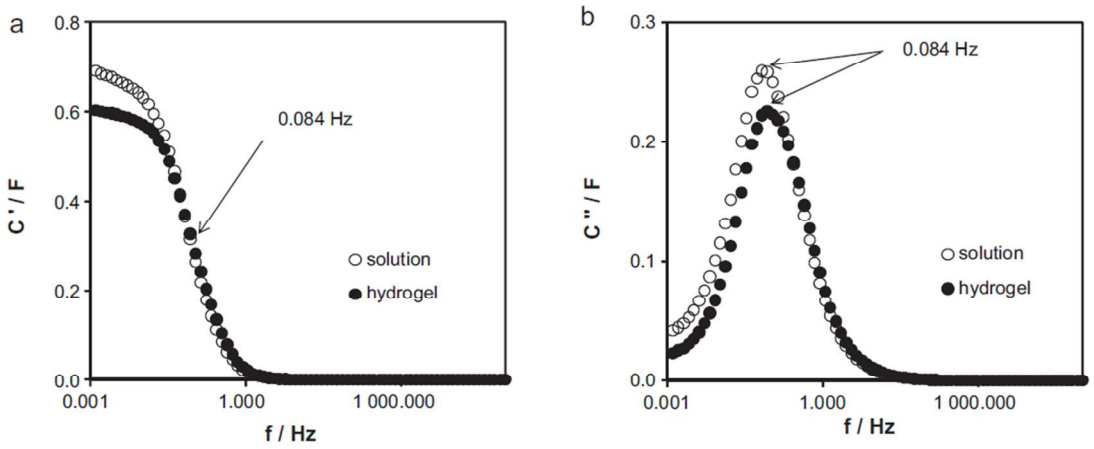

Fig. 12 Comparison of EDLC cell with a polymer hydrogel electrolyte and aqueous H_2SO_4 solution: (a) real part of capacitance vs. frequency; and (b) imaginary part of capacitance vs. frequency. Reprinted with permission from Stepniak and Ciszewski.[128] Copyright 2011 Elsevier.

Kalupson *et al.* demonstrated a flexible EDLC enabled by a GA cross-linked PVA hydrogel with an 1 M or 3 M H_2SO_4 electrolyte and binder-free SWCNT electrodes.[129] Both pristine and oxidized (to introduce pseudo-capacitance) SWCNTs were used to fabricate a flexible device. These ultra-thin EDLCs displayed a very high rate performance with a 15 ms time constant and almost no reduction in performance after 10,000 cycles.

Table 8 Summary of acidic hydrogel EDLCs reported in the literature

Polymer host	Ionic conductor	Proton conductivity (Scm^{-1})	Electrolyte production method	Cell design	Testing/storage environment	Electrode active material	Cell capacitance	Ref.
GA cross-linked PVA	1 M H_2SO_4	2.6×10^{-1} (from [124])	Free-standing film	Sandwiched	Room temperature	Activated carbon fiber cloths	33 Fg^{-1} (at 1 $mAcm^{-2}$)	122
GA cross-linked PVA	4 M H_2SO_4	6×10^{-1}	Free-standing film	Sandwiched	Room temperature	Activated carbon fiber cloths	42 Fg^{-1} (at 1 $mAcm^{-2}$)	124
GA cross-linked PVA	2M $HClO_4$	ca. 1×10^{-3}	Free-standing film	Sandwiched	Room temperature, 100% RH	Black pearl carbon	97 Fg^{-1} (at 0.5 $mAcm^{-2}$)	125
Cellulose/chitin blend	2 M H_2SO_4 and ionic liquids	5.78×10^{-1}	Free-standing film	Sandwiched	Room temperature	Activated carbon fiber cloths	162 Fg^{-1} (at 5000 mAg^{-1})	127
GA cross-linked PVA/PAA blend	1.5 M $HClO_4$	1×10^{-3} – 1×10^{-2}	Free-standing film	Sandwiched	Room temperature	Black pearl carbon	60 Fg^{-1} (at 2 mVs^{-1})	126
PAAM	3.7 M H_2SO_4	6.9×10^{-1}	Separator impregnated with hydrogel	Sandwiched	Room temperature	Activated carbon fiber cloths	142 Fg^{-1} (at 10 mVs^{-1})	128
GA cross-linked PVA	1 or 3 M H_2SO_4	4.5×10^{-2} †	Free-standing film	Sandwiched	Room temperature	SWCNT	13 Fg^{-1} (at 10^{-3} Hz)	129
GA cross-linked PVA	1 M or 3 M H_2SO_4	4.5×10^{-2} †	Free-standing film	Sandwiched	Room temperature	Oxidized SWCNT	23 Fg^{-1} (at 10^{-3} Hz)	129

* Estimated from charge-discharge curve
† Containing 1 M H_2SO_4

4.2.2 Pseudo-capacitors

Acidic hydrogels have also been investigated as polymer electrolytes for pseudo-capacitors (Table 9). As discussed earlier, a GA cross-linked PVA/PAA blend with 1.5 M $HClO_4$ was used as a hydrogel electrolyte.[126] Utilizing a $RuO_x \cdot nH_2O$/carbon electrode, a solid pseudo-capacitor exhibited a capacitance of 1,000 Fg^{-1} at a 2 mVs^{-1} scan rate. However this device suffered from a significant reduction in capacitance after 45 cycles. In a more recent study, different acrylic gel polymer electrolytes, including PAA, potassium polyacrylate (PAAK), and poly(2-acrylamido-2-methyl-1-propanesulfonic acid) (PAMPS), were used for RuO_2 pseudo-capacitors.[130] The RuO_2/Pt electrode in PAMPS showed higher capacitance than in 1 M H_2SO_4 (642 Fg^{-1} vs. 596 Fg^{-1} electrode capacitance). This may be due to better proton accommodation in the polymer side chain groups.

4.2.3 Further improvements

Since acidic hydrogels exhibit low adhesion to the electrode surface, mechanical pressure is required to ensure good interfacial contact between the electrode and electrolyte in an assembled cell. This often adds extra volume, weight and other complexities to the devices, which needs to be addressed. In addition, the life time and shelf life of acidic hydrogel supercapacitors (both EDLCs and pseudo-capacitors) have not been extensively studied and the long-term performance under operating conditions is unknown. Since the main content of these hydrogel polymer electrolytes is in a quasi-liquid state, preventing the cell from "drying" for long term storage is another major challenge. The loosely bonded and/or free water molecules in the hydrogels undergo fast dehydration, which significantly affects the conductivity of the electrolyte. For

supercapacitors that operate in an ambient environment, water retention is critical. Alternatively, other inorganic hydrogels, such as sol-gels or fumed SiO_2 gels, have also been developed for supercapacitors[131-134] and shown promise of improved device performance.

Table 9 Summary of acidic hydrogel pseudo-capacitors reported in the literature.

Polymer host	Ionic conductor	Proton conductivity (Scm^{-1})	Electrolyte production method	Cell design	Testing/storage environment	Electrode active material	Cell capacitance	Ref.
GA cross-linked PVA/PAA blend	1.5 M $HClO_4$	10^{-3}–10^{-2}	Free-standing film	Sandwiched	Room temperature	$RuO_x \cdot nH_2O$ /Carbon	1,000 Fg^{-1} (at 2 mVs^{-1})	126
PAMPS	1 M H_2SO_4	2.1×10^{-2}	-	3-electrode system	-	RuO_2/Pt	418 Fg^{-1} (at 20 mVs^{-1})†	130
PAA	1 M H_2SO_4	2.3×10^{-2}	-	3-electrode system	-	RuO_2/Pt	521 Fg^{-1} (at 20 mVs^{-1})†	130
PAAK	1 M H_2SO_4	1.8×10^{-2}	-	3-electrode system	-	RuO_2/Pt	464 Fg^{-1} (at 20 mVs^{-1})†	130

† Single electrode capacitance

4.3 Heteropolyacids/polymer composite electrolytes

With the development of solid-state proton conductors, polymer-in-salt electrolytes have shown promising performance. The majority content of a polymer-in-salt electrolyte is the solid ionic conductor, which is embedded in a polymer matrix. Due to the low polymer content, the ionic conduction mechanism is similar to its pure solid counterpart and often obeys an Arrhenius-type dependence.

Heteropolyacids (HPAs) are hydrous salts and have the highest proton conductivity at room temperature among inorganic solid-state proton conductors.[135-139] Two common HPAs are silicotungstic acid (SiWA, $H_4SiW_{12}O_{40}$) and phosphotungstic acid (PWA, $H_3PW_{12}O_{40}$). Due to their high proton conductivity, HPAs have been used to modify PFSA membranes.[140, 141] Two major factors contribute to their proton conductivity: (i) Highly hydrogen-bonded conduction pathways in the crystal lattice facilitate fast proton transportation. Such pathways result from a large number of crystallized water molecules in the crystal hydrate (e.g. SiWA•nH_2O), leading to "quasi-liquid" states.[139, 142, 143] (ii) The dynamic dissociation of co-crystallized water molecules in the crystal hydrate via interactions with oxygen atoms of the Keggin anion increases the density of free protons. The protons, in the forms of H^+-nH_2O clusters (e.g. H_3O^+ or $H_5O_2^+$), are transferred by hopping from H^+-nH_2O donor sites to nH_2O acceptors in the HPA, yielding high proton conductivity (e.g. 0.027 Scm^{-1} for SiWA•$28H_2O$).[136]

Studies have identified the temperature and RH dependence of the number of crystalized water molecules in HPAs.[143, 144] Their activation energy increases as the number of crystallized water molecule decreases.[135] Although HPA crystals tend to dehydrate when being heated or when in an atmosphere with low RH (leading to a

reduction in proton conductivity[137]), they can easily rehydrate when they are in a high RH environment following dehydration.

Several HPA-in-polymer composite electrolyte systems have been demonstrated for both EDLCs and pseudo-capacitors. The addition of the polymer increases the resilience of HPA to changes in RH. Although the diffusion of the HPA species may be limited once immobilized in the polymer matrix, this negative effect can be minimized thorough different additives and modifications to the polymer matrix.

4.3.1 Electrochemical double layer capacitors and pseudo-capacitors

For HPA/polymer composite systems, PVA is typically chosen as polymer matrix. A mixture of 90 wt. % SiWA and 10 wt. % PVA (referred to as SiWA-PVA) has exhibited a proton conductivity of 0.01 Scm^{-1} at room temperature, and has been successfully applied in RuO_2 pseudo-capacitors.[145] The capacitance of the solid device was lower than the capacitance of a similar capacitor with an aqueous electrolyte (50 $mFcm^{-2}$ vs. 70 $mFcm^{-2}$), which was due to ionic penetration in the solid-state. Nevertheless, the solid capacitor was able to be charged and discharged at 1 Vs^{-1}, showing a high rate capability. In addition, the solid SiWA-PVA electrolyte-enabled capacitor exhibited good shelf life and good cycle life (over 20,000 cycles).

A PWA-PVA polymer electrolyte was demonstrated in a RuO_2/graphite asymmetric pseudo-capacitor.[146] The device was only 0.2 mm thick and had a 1.5 V working voltage window. Two distinct capacitive regions (the first region from 0 to 0.7 V and the second from 0.7 to 1.55 V) were identified in the CV. Both showed a symmetric and reversible nature, but the former was dominated by the double-layer electrode with a capacitance of 2 $mFcm^{-2}$, while the latter demonstrated a 10-fold increase in capacitance

to about 22 $mFcm^{-2}$. The presence of these two voltage regions was confirmed in charge/discharge experiments. The HPA not only provided proton conductivity, but also contributed to pseudo-capacitance in the operating voltage window due the redox reactions of its anions.[147]

To further optimize proton conductivity, SiWA-PVA and PWA-PVA were combined together into a single composite electrolyte.[148, 149] The mixture of PWA and SiWA exhibited higher conductivity than its individual components at equivalent concentration. A solid RuO_2 pseudo-capacitor enabled by a SiWA-PWA-PVA polymer electrolyte was able to deliver a capacitance of 50 $mFcm^{-2}$ at 500 mVs^{-1} without distortion in its CV.[148] Since PWA is more sensitive to dehydration than SiWA, the resultant SiWA-PWA-PVA polymer electrolyte suffered a reduction in conductivity in RH conditions below 30 % RH. In addition, although the high HPA content enhances proton conductivity, it also leads to a deterioration of mechanical properties, which in turn limits the mechanical flexibility of the solid capacitors.

A ternary complex was developed to replace the rigid or even brittle HPA-PVA binary complex by introducing a limited amount of H_3PO_4 into the system.[150, 151] Pure H_3PO_4 has the highest intrinsic proton conductivity of any compound.[152, 153] An H_3PO_4/PVA anhydrous system has been successfully demonstrated as an acid/polymer blend electrolyte. H_3PO_4 acts as a plasticizer as well as an additional proton donor. The addition of H_3PO_4 also promoted the retention of crystallized water as well as the thermal stability of the polymer electrolyte.[151] The first solid supercapacitor based on SiWA-H_3PO_4-PVA was demonstrated using conductive graphite electrodes.[150, 151] The solid EDLC showed good high rate capability to be charged and discharged at 20 Vs^{-1} in the

CV and a time constant of 10 ms. A molybdenum nitride (Mo_xN) pseudo-capacitor was also developed[154] and delivered 1 $mFcm^{-2}$ at 100 Vs^{-1} while achieving a 10 ms time constant. In addition, textile EDLCs based on knitted carbon fibers and activated carbon ink were demonstrated with 510 $mFcm^{-2}$ at 10 mVs^{-1}.[155] The flexible EDLC device was stretched about 50% and was bent up to 180° several times and still remained functional.

Due to the moisture sensitivity of HPA, the conductivity of SiWA-H_3PO_4-PVA fluctuates with RH at room temperature. The environmental stability of the polymer electrolyte was improved by the incorporation of inorganic nano-fillers[156] and chemically cross-linking of the PVA polymer[157]. The addition of nano-SiO_2 fillers enhanced the water retention of SiWA-H_3PO_4-PVA. This electrolyte exhibited improved environmental stability due to the additional hydrogen bonds formed between SiO_2 and water molecules. A cross-linking effect of SiO_2 on PVA was also confirmed via IR spectroscopy as a secondary function. The degree of chemical cross-linking of the PVA framework was optimized to improve the water storage capability and dimensional stability of SiWA-H_3PO_4-PVA. The resultant electrolyte exhibited enhanced proton conductivity via a hopping mechanism and could transfer ions at an ultra-high speed. The electrolyte film showed high mechanical flexibility in both dried and hydrated conditions, as shown in Fig. 13. Thermal analysis revealed an increase of water content with increasing degree of cross-link, such that SiWA in the cross-linked polymer electrolyte had a higher level of hydration. IR analysis confirmed stronger hydrogen bonding interaction due to hydrated SiWA.

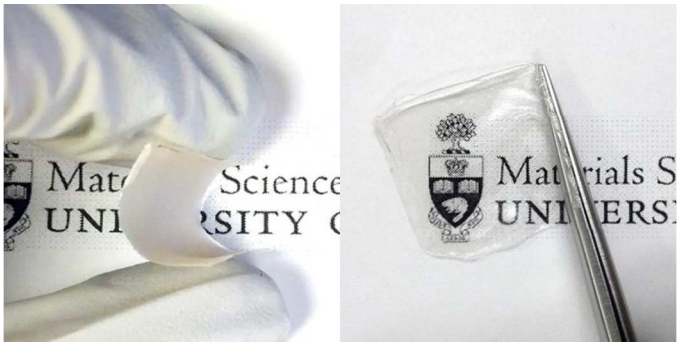

Fig. 13 Photographs of a cross-linked SiWA-H_3PO_4-PVA electrolyte film in dried (left) and hydrated (right) conditions.

The resultant cross-linked SiWA-H_3PO_4-PVA electrolyte is capable of storing and delivering charge at an ultrahigh rate and retaining its conductivity and ultrahigh rate capability over time. Fig. 14 shows a comparison of three metallic EC devices, 30 wt% H_2SO_4 (liquid cell), Nafion (solid cell), and cross-linked SiWA-H_3PO_4-PVA (solid cell), with planar stainless steel electrodes at a voltage scan rate of 5000 Vs^{-1} at the same RH. All cells were able to charge and discharge at this ultra-high scan rate, but the solid SiWA-H_3PO_4-PVA based device appeared to have less resistance and higher capacitance than the other cells. At such high rate, the cell using cross-linked SiWA-H_3PO_4-PVA was able to deliver 10 μFcm^{-2}, 50% of the capacitance obtained at 1 Vs^{-1}.

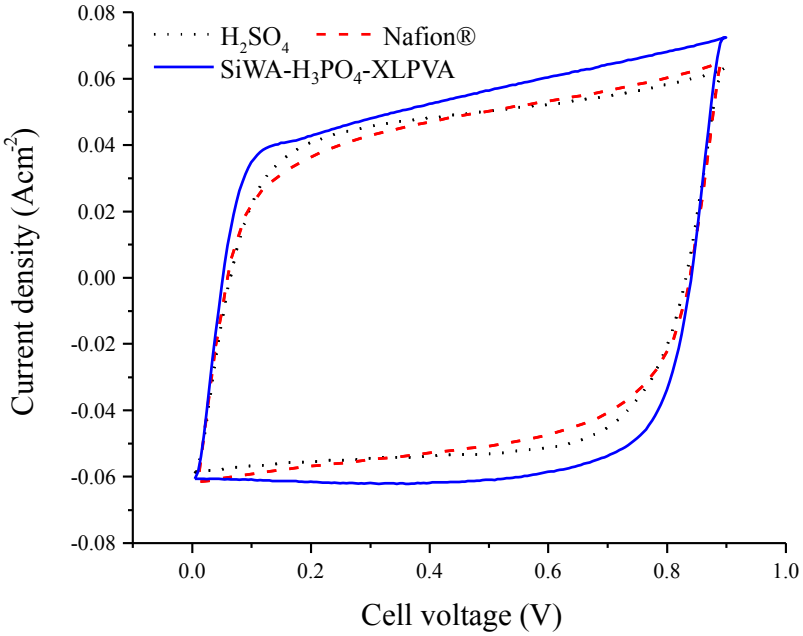

Fig. 14 CVs of thin metallic EC cells with 30 wt.% H_2SO_4, Nafion, and cross-linked SiWA-H_3PO_4-PVA electrolytes at a scan rate of 5000 Vs^{-1}.

Graphite EDLCs enabled by cross-linked SiWA-H_3PO_4-PVA exhibited a high capacitance of 2 $mFcm^{-2}$ at 50 Vs^{-1} and a time constant of 10 ms. Fig. 15 shows the CVs of the solid device at scan rates of 1, 10, 25, and 50 Vs^{-1}. The capacitance at 1 Vs^{-1} was about 2.5 $mFcm^{-2}$ higher than an onion-like nanocarbon-based liquid EC[158] and graphene-based liquid and solid ECs[9, 101, 159]. A further increase in scan rate resulted in only a slight decrease of capacitance to 2 $mFcm^{-2}$ at 50 Vs^{-1}, which is among the highest areal capacitance for supercapacitors at this rate, liquid or solid.

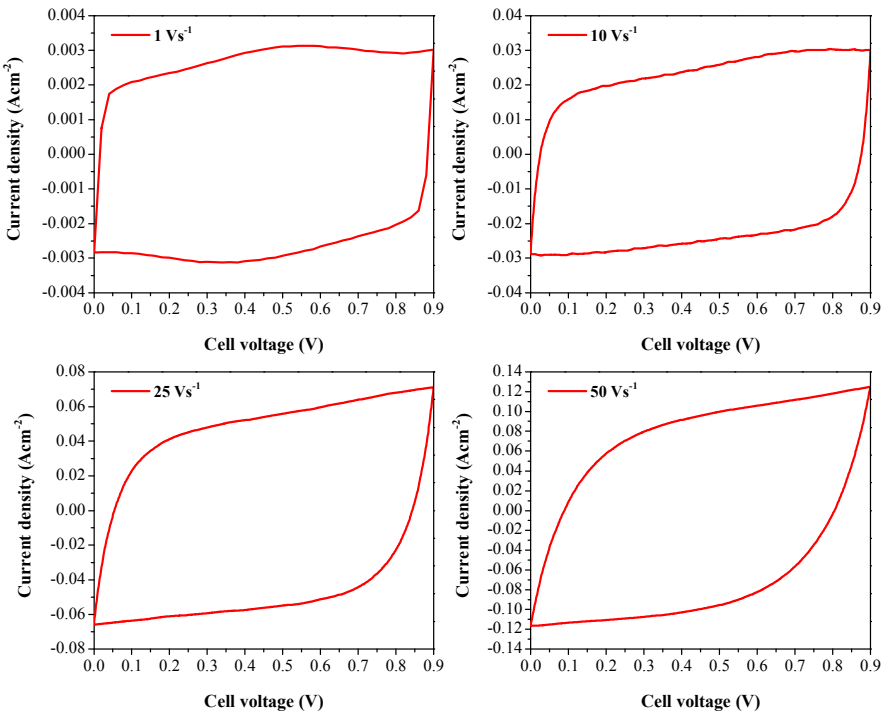

Fig. 15 CVs of a thin graphite EDLC with a cross-linked SiWA-H_3PO_4-PVA electrolyte at sweep rates of 1 Vs^{-1}, 10 Vs^{-1}, 25 Vs^{-1}, and 50 Vs^{-1}. Reprinted with permission from Gao and Lian.[157] Copyright 2012 Royal Society of Chemistry.

4.3.2 Further improvements

SiWA-PVA solid polymer electrolyte systems are very promising for high-rate and high-power energy storage devices. Current effort is on further enhancing solid-state proton conductivity, environmental stability (e.g. for RH < 30%), and the electrochemical stability window. However, improvements of individual characteristics are much easier to achieve than jointly satisfying all goals. For example, hygroscopic additives can aid water retention within HPA crystals and electrolytes; however, they may negatively affect proton conductivity. HPA salts, through cation exchange, may also be an effective way to increase the environmental stability of the electrolytes. Moreover, HPA salts with larger cations (e.g. cesium or ammonium salts), in spite of containing less crystallized water, exhibit less dependence on RH.[139] Although such salts will have reduced ionic conductivity, this decrease in conductivity may be acceptable and relatively minor compared to their overall benefit. Consequently, the development of HPA-based polymer electrolytes will need to be application specific and require a balanced approach.

Table 10 Summary of HPA/polymer composite electrolyte-based EDLCs and pseudo-capacitors.

Polymer electrolyte	HPA Wt.% in the composite*	Proton conductivity (Scm^{-1})	Electrolyte production method	Cell design	Testing/storage environment	Electrode active material	Cell capacitance	Ref.
SiWA-PVA	90 wt.%	1×10^{-2}	Solution casting on electrodes	Sandwiched with hot pressing	Room temperature	RuO_2/Ti	50 $mFcm^{-2}$ (at 0.1 Hz)	145
PWA-PVA	87 wt.%	-	Solution casting on electrodes	Sandwiched with hot pressing	Room temperature	Positive: RuO_2/Ti Negative: Graphite	ca. 15 $mFcm^{-2}$ (at 100 mVs^{-1}) †	146
SiWA-PWA-PVA	45 wt.% SiWA; 45 wt.% PWA	1.3×10^{-2}	Solution casting on electrodes	Sandwiched with hot pressing	Room temperature	RuO_2/Ti	50 $mFcm^{-2}$ (at 500 mVs^{-1})	149
SiWA-H_3PO_4-PVA	65 wt.%	8×10^{-3}	Solution casting on electrodes	Sandwiched with hot pressing	Room temperature	Graphite	1 $mFcm^{-2}$ (at 1 Vs^{-1})	150
SiWA-H_3PO_4-PVA	80 wt.%	1×10^{-2}	Solution casting on electrodes	Sandwiched with hot pressing	Room temperature	Graphite	1 $mFcm^{-2}$ (at 1 Vs^{-1})	151
SiWA-H_3PO_4-PVA	80 wt.%	ca.1.3×10^{-2}	Solution casting on electrodes	Sandwiched with hot pressing	Room temperature	Mo_xN/Ti	1 $mFcm^{-2}$ (at 100 Vs^{-1})	154
SiWA-H_3PO_4-PVA	-	-	Solution casting on electrodes	Sandwiched with hot pressing	Room temperature	Carbon fibers and activated carbon	510 $mFcm^{-2}$ (at 10 mVs^{-1})	155

Polymer electrolyte	HPA Wt.% in the composite*	Proton conductivity (Scm^{-1})	Electrolyte production method	Cell design	Testing/storage environment	Electrode active material	Cell capacitance	Ref.
Cross-linked SiWA-H_3PO_4-PVA	85 wt.%	ca.1.5×10^{-2}	Solution casting on electrodes/ Free-standing film	Sandwiched with pressing	Room temperature	Graphite	2 $mFcm^{-2}$ (at 50 Vs^{-1})	157

* Calculated based on dried HPA/polymer film
† Calculated from CV

5 Summary and outlook

With the current advances in printed electronics, wearable electronics, and e-textiles, solid, energy storage systems that are light-weight, thin, and flexible are facing tremendous opportunities. Beyond offering the required form factors, supercapacitors can be stand-alone or form hybrids with batteries or solar cells to provide high performance, high power, and low maintenance energy solutions. Utilizing polymer electrolytes will be particularly beneficial in these next generation supercapacitors. Polymer electrolytes can prevent leakage, minimize sealing or packaging processes, and provide more functionality for device fabrication. Although the conductivity of polymer electrolytes is typically a few orders of magnitude lower than that of their liquid counterparts, deploying them in the form of very thin films helps to overcome the problems associated with their inherently low intrinsic proton conductivity. Short and consistent proton-conducting paths within a thin electrolyte film can enable good conductivity.

This review emphasized state-of-the-art research on low to room temperature proton-conducting polymer electrolytes, with a particular focus on both polymeric proton-conducting and inorganic/polymer proton-conducting electrolytes and the supercapacitors enabled by these electrolytes. Table 11 briefly summaries the advantages and disadvantages of the proton-conducting polymer electrolytes discussed in this review. Identified shortcomings in the current technologies point to directions for further improvement:

i. *Proton conductivity and pseudo-capacitance*. A major challenge remains to increase the proton conductivity in low temperature and/or low RH environments. Modifications to the electrolyte film in order to improve its water retention

capability and to reduce the sensitivity to the environment are essential. The effects of different hygroscopic materials or plasticizers on environmental stability should be identified and tested. The addition of a redox active mediator into the polymer electrolytes may further enhance cell capacitance. A balance between reaction kinetics and ion mobility is critical to reach optimum capacitor performance.

ii. *Voltage window*. Although the cell voltage of aqueous-based flexible supercapacitors is limited to around 1 V, the design of supercapacitors with high energy density is ongoing. Asymmetric cell configurations promise to increase the voltage window and further enhance the energy density of the supercapacitors. The development of protic ionic liquids may further benefit this field by opening up the voltage window limit. However, one needs to overcome the low ionic conductivity (dissociation and mobility) of ionic liquids for any practical high power applications.

iii. *Electrode-electrolyte interface*. The interface between solid electrodes and electrolyte is a critical issue. Earlier research was focused on free-standing electrolyte films. Flexible solid supercapacitors can also be produced by (i) direct solution casting of the polymer electrolyte solution onto the electrode surface or (ii) dip-coating of the electrodes in the polymer electrolyte solution. Although these approaches minimize the interfacial contact resistance, the properties of the polymer electrolyte liquid precursor solution have not been widely studied and optimized. Few studies are devoted to the electrode/electrolyte interface, starting from the gel form to the solidified form of the electrolyte. More fundamental

work is needed to fully understand the ion transport in polymer electrolytes and their interaction with electrode materials to maximize ion mobility while minimizing self-discharge.

iv. *Processing and Integration techniques:* Among the main drivers of printed and flexible electronics are the low cost of materials and high through-put processes. The majority of inorganic/polymer proton-conducting electrolytes are relative inexpensive, which is highly desirable for scale-up and commercialization. To be compatible with and able to be integrated with printed electronics, wearable electronics, and micro-electronics, the design and development of polymer electrolytes needs to also consider the material properties, such as viscosity, curing conditions, and chemical compatibility with the printing equipment (e.g., screen printing, gravure printing) for processability and manufacturability.

v. *Electrolyte film mechanical properties*. While extensive work has been performed on non-stretchable flexible supercapacitors, stretchable supercapacitors may further improve the practicality of wearable applications. This requires electrolyte films that can be plastically or non-plastically deformed. Studies of polymer electrolytes are still in an initial stage, focusing on electrochemical performance, while less attention is paid to mechanical properties. Theoretical and computational modeling can be effective in predicting and optimizing the mechanical properties of electrolytes.

vi. *Performance metric*. Lastly, it is difficult to directly compare capacitor performance between different studies, since for flexible solid supercapacitors performance should be normalized by geometric area or volume instead of the

mass of the active materials, as is current practice. Unfortunately, in current studies we find diverse metrics, even such based on the weight of the electrodes themselves rather than the active material only. It is necessary to establish consistent and clear rules for performance evaluation. It is also important to establish evaluation criteria that represent practical applications, such as outdoors or at extreme temperatures.

There are many promising chemistries for solid supercapacitors, but scale-up and commercialization still need to overcome many hurdles. Researchers are continuing to push the performance of materials and new chemistries, but system development is equally important and requires a comprehensive approach and multi-disciplinary efforts. The current rapid pace of development in high performance materials coupled with expertise in system integration will speed up the realization of next generation supercapacitors.

Table 11. Comparison between of different proton-conducting polymer electrolytes

	Perfluorosulphonic acids	Sulfonated hydrocarbons	Acid/polymer blends	Acidic hydrogels	Heteropolyacids/ polymer composites
Ambient proton conductivity	Low	Low	Medium to low	High	High
Environmental stability	Low	Low	High to medium	Low	Medium
Ease of preparation	High	Medium	High	Medium	Medium
Chemical stability	High	High	Medium	Medium	High
Thin-film processability	High	High	Medium to low	Low	High
Cost	High	Medium	Low	Low	Medium

List of abbreviations

CNT	carbon nanotube
CV	cyclic voltammograms
DEC	diethyl carbonate
DMA	dimethyl amine
DMAC	dimethyl acetamide
DMF	dimethyl formamide
EC	ethylene carbonate
EDLC	electrochemical double layer capacitor
EIS	electrochemical impedance spectroscopy
ESR	equivalent series resistance
GA	glutaraldehyde
HPA	heteropolyacids
HUP	hydrogen uranyl phosphate
MEMS	microelectromechanical systems
MWCNT	multi-wall carbon nanotube
P2VP	poly(2-vinylpyridine)
P4VP	poly(4-vinylpyridine)
PAA	poly(acrylic acid)
PAAK	potassium polyacrylate
PAAM	poly(acrylamide)
PAMPS	poly(2-acrylamido-2-methyl-1-propanesulfonic acid)
PAN	poly(acrylonitrile)
PANI	polyaniline
PBI	polybenzimidazole
PC	propylene carbonate
PEEK	poly(ether ether ketone)
PEEKK	poly(ether ether ketone ketone)
PEK	poly(ether ketones)
PEO	poly(ethylene oxide)
PES	poly(ether sulfones)
PFENO	poly(fluorenyl ether nitrile oxynaphthalate)
PFSA	perfluorosulphonic acid
PMA	polymethacrylate
PMMA	poly(methylmethacrylate)
PPy	polypyrrole
PSS	poly(styrene-4-sulphonate)
PTFE	polytetrafluorethylene
PVA	poly(vinyl alcohol)
PVP	poly(vinylpyrrolidone)
RH	relative humidity
SWCNT	single-wall carbon nanotube
VTF	Vögel-Tamman-Fulcher

Acknowledgments

We appreciate the financial support from NSERC Canada. H. Gao would like to acknowledge an NSERC Alexander Graham Bell Canada Graduate Scholarship and a Hatch Graduate Scholarship for Sustainable Energy Research.

References

1. B. E. Conway, *Electrochemical supercapacitors: scientific fundamentals and technological applications*, Springer, New York, 1999.
2. B. Conway and W. Pell, *J. Solid State Electrochem.*, 2003, **7**, 637-644.
3. A. Burke, *J. Power Sources*, 2000, **91**, 37-50.
4. H. I. Becker, U. S. Patents, US2800616, U.S., 1957
5. P. Simon and Y. Gogotsi, *Nat Mater*, 2008, **7**, 845-854.
6. P. Simon and Y. Gogotsi, *Acc. Chem. Res.*, 2012, **46**, 1094-1103.
7. L. L. Zhang and X. S. Zhao, *Chem. Soc. Rev.*, 2009, **38**, 2520-2531.
8. M. Beidaghi and Y. Gogotsi, *Energy Environ. Sci.*, 2014, **7**, 867-884.
9. J. R. Miller, R. Outlaw and B. Holloway, *Science*, 2010, **329**, 1637-1639.
10. Z.-S. Wu, X. Feng and H.-M. Cheng, *National Science Review*, 2013.
11. Y. B. Tan and J.-M. Lee, *J. Mater. Chem. A*, 2013, **1**, 14814-14843.
12. T. Chen and L. Dai, *J. Mater. Chem. A*, 2014.
13. X. Cai, M. Peng, X. Yu, Y. Fu and D. Zou, *J. Mater. Chem. C*, 2014, **2**, 1184-1200.
14. Y. Gogotsi and P. Simon, *Science*, 2011, **334**, 917-918.
15. Y.-D. Chiou, D.-S. Tsai, H. H. Lam, C.-h. Chang, K.-Y. Lee and Y.-S. Huang, *Nanoscale*, 2013, **5**, 8122-8129.
16. H.-K. Kim, S.-H. Cho, O. Young-Woo, T.-Y. Seong and Y. S. Yoon, *Journal of Vacuum Science & Technology B: Microelectronics and Nanometer Structures*, 2003, **21**, 949-952.
17. H. Gao, J. Li and K. Lian, *RSC Advances*, 2014, **4**, 21332-21339.
18. C.-C. Yang, S.-T. Hsu and W.-C. Chien, *J. Power Sources*, 2005, **152**, 303-310.
19. L. M. Miller, P. K. Wright, C. C. Ho, J. W. Evans, P. C. Shafer and R. Ramesh, in *Energy Conversion Congress and Exposition, 2009. ECCE 2009. IEEE*, 2009, pp. 2627-2634.
20. K. Yu Jin, C. Haegeun, H. Chi-Hwan and K. Woong, *Nanotechnology*, 2012, **23**, 065401.
21. M. F. El-Kady and R. B. Kaner, *Nat Commun*, 2013, **4**, 1475.
22. S. Ketabi, Z. Le and K. Lian, *Electrochem. Solid-State Lett.*, 2011, **15**, A19-A22.
23. S. Ketabi and K. Lian, *Electrochim. Acta*, 2013, **103**, 174-178.
24. W. E. Ayrton and P. John, *Proc. Phys. Soc. London*, 1875, **2**, 171-182.
25. N. Bjerrum, *Science*, 1952, **115**, 385-390.
26. M. L. Di Vona and P. Knauth, in *Solid State Proton Conductors*, John Wiley & Sons, Ltd, 2012, pp. 1-4.
27. P. Colomban, *Proton Conductors: Solids, membranes and gels-materials and devices*, Cambridge University Press, 1992.
28. J. Beintema, *Recl. Trav. Chim. Pays-Bas*, 1938, **57**, 155-175.
29. W. T. Grubb, *J. Electrochem. Soc.*, 1959, **106**, 275-278.
30. W. T. Grubb and L. W. Niedrach, *J. Electrochem. Soc.*, 1960, **107**, 131-135.
31. A. Baranov, L. Shuvalov and N. Shchagina, *JETP lett*, 1982, **36**, 459-462.
32. G. Alberti and E. Torracca, *J. Inorg. Nucl. Chem.*, 1968, **30**, 1093-1099.
33. J. T. Kummer, *Prog. Solid State Chem.*, 1972, **7**, 141-175.

34. J. C. Lassegues, B. Desbat, O. Trinquet, F. Cruege and C. Poinsignon, *Solid State Ionics*, 1989, **35**, 17-25.
35. A. J. Polak, S. Petty-weeks and A. J. Beuhler, *Sens. Actuators*, 1986, **9**, 1-7.
36. S. Petty-Weeks and A. J. Polak, *Sens. Actuators*, 1987, **11**, 377-386.
37. O. Nakamura, T. Kodama, I. Ogino and Y. Miyake, *Chem. Lett.*, 1979, **8**, 17-18.
38. J. Livage, *Solid State Ionics*, 1992, **50**, 307-313.
39. C. A. Linkous, *Int. J. Hydrogen Energy*, 1993, **18**, 641-646.
40. B. R. Breslau and I. F. Miller, *Ind. Eng. Chem. Res.*, 1971, **10**, 554-565.
41. K. D. Kreuer, S. J. Paddison, E. Spohr and M. Schuster, *Chem. Rev.*, 2004, **104**, 4637-4678.
42. C. v. Grotthuss, *Ann. Chim. (Paris)*, 1806, **LVIII** 54-73.
43. N. Agmon, *Chem. Phys. Lett.*, 1995, **244**, 456-462.
44. K. D. Kreuer, *Chem. Mater.*, 1996, **8**, 610-641.
45. F. M. Gray, *Solid Polymer Electrolytes: Fundamentals and Technological Applications*, Wiley, 1991.
46. M. Maréchal, J. L. Souquet, J. Guindet and J. Y. Sanchez, *Electrochem. Commun.*, 2007, **9**, 1023-1028.
47. S. Slade, S. Campbell and T. Ralph, *J. Electrochem. Soc.*, 2002, **149**, A1556-A1564.
48. J. Sumner, S. Creager, J. Ma and D. DesMarteau, *J. Electrochem. Soc.*, 1998, **145**, 107-110.
49. P. Staiti, M. Minutoli and F. Lufrano, *Electrochim. Acta*, 2002, **47**, 2795-2800.
50. F. Lufrano, P. Staiti and M. Minutoli, *J. Power Sources*, 2003, **124**, 314-320.
51. F. Lufrano and P. Staiti, *Electrochim. Acta*, 2004, **49**, 2683-2689.
52. P. Staiti and F. Lufrano *J. Electrochem. Soc.*, 2005, **152**, A617-A621.
53. C. S. Ramya, C. K. Subramaniam and K. S. Dhathathreyan, *J. Electrochem. Soc.*, 2010, **157**, A600-A605.
54. C. K. Subramaniam, C. S. Ramya and K. Ramya, *J. Appl. Electrochem.*, 2011, **41**, 197-206.
55. B. G. Choi, J. Hong, W. H. Hong, P. T. Hammond and H. Park, *ACS Nano*, 2011, **5**, 7205-7213.
56. C. Huang and P. S. Grant, *Sci. Rep.*, 2013, **3**, 2393.
57. D. P. Cole, A. L. M. Reddy, M. G. Hahm, R. McCotter, A. H. C. Hart, R. Vajtai, P. M. Ajayan, S. P. Karna and M. L. Bundy, *Adv. Energy Mater.*, 2014, **4**, 1300844.
58. J. H. Chang, J. H. Park, G. G. Park, C. S. Kim and O. O. Park, *J. Power Sources*, 2003, **124**, 18-25.
59. P. Staiti and F. Lufrano, *Electrochim. Acta*, 2007, **53**, 710-719.
60. S. Sarangapani, P. Lessner, J. Forchione, A. Griffith and A. B. Laconti, *J. Power Sources*, 1990, **29**, 355-364.
61. A. B. LaConti, P. M. Lessner and S. Sarangapani, U. S. Patents, US5136474, 1992
62. K.-W. Park, H.-J. Ahn and Y.-E. Sung, *J. Power Sources*, 2002, **109**, 500-506.
63. X. Liu and P. G. Pickup, *Energy Environ. Sci.*, 2008, **1**, 494-500.
64. P. G. Pickup, C. L. Kean, M. C. Lefebvre, G. Li, Z. Qi and J. Shan, *J. New Mater. Electrochem. Syst.*, 2000, **3**, 21-26.

65. A. M. White and R. C. T. Slade, *Synth. Met.*, 2003, **139**, 123-131.
66. P. Staiti and F. Lufrano, *Electrochim. Acta*, 2010, **55**, 7436-7442.
67. A. Leela Mohana Reddy, F. Estaline Amitha, I. Jafri and S. Ramaprabhu, *Nanoscale Res. Lett.*, 2008, **3**, 145-151.
68. B. Baradie, J. Dodelet and D. Guay, *J. Electroanal. Chem.*, 2000, **489**, 101-105.
69. K. Kanamura, T. Mitsui and H. Munakata, *Chem. Mater.*, 2005, **17**, 4845-4851.
70. J. D. Halla, M. Mamak, D. E. Williams and G. A. Ozin, *Adv. Funct. Mater.*, 2003, **13**, 133-138.
71. Z.-G. Shao, P. Joghee and I. M. Hsing, *J. Membr. Sci.*, 2004, **229**, 43-51.
72. A. S. Aricò, V. Baglio, A. Di Blasi, P. Creti, P. L. Antonucci and V. Antonucci, *Solid State Ionics*, 2003, **161**, 251-265.
73. R. Claire Greaves, S. P. Bond and W. R. McWhinnie, *Polyhedron*, 1995, **14**, 3635-3639.
74. C. Felice and D. Qu, *Industrial & Engineering Chemistry Research*, 2010, **50**, 721-727.
75. R. Nagarale, G. Gohil and V. K. Shahi, *J. Membr. Sci.*, 2006, **280**, 389-396.
76. J. Roeder, V. Zucolotto, S. Shishatskiy, J. R. Bertolino, S. P. Nunes and A. T. N. Pires, *J. Membr. Sci.*, 2006, **279**, 70-75.
77. J. Yang, P. K. Shen, J. Varcoe and Z. Wei, *J. Power Sources*, 2009, **189**, 1016-1019.
78. F. Meng, N. V. Aieta, S. F. Dec, J. L. Horan, D. Williamson, M. H. Frey, P. Pham, J. A. Turner, M. A. Yandrasits, S. J. Hamrock and A. M. Herring, *Electrochim. Acta*, 2007, **53**, 1372-1378.
79. K. D. Kreuer, *J. Membr. Sci.*, 2001, **185**, 29-39.
80. D.-W. Kim, J. M. Ko, W. J. Kim and J. H. Kim, *J. Power Sources*, 2006, **163**, 300-303.
81. W. J. Kim and D.-W. Kim, *Electrochim. Acta*, 2008, **53**, 4331-4335.
82. Y.-H. Seong, N.-S. Choi and D.-W. Kim, *Electrochim. Acta*, 2011, **58**, 285-289.
83. G. Wee, O. Larsson, M. Srinivasan, M. Berggren, X. Crispin and S. Mhaisalkar, *Adv. Funct. Mater.*, 2010, **20**, 4344-4350.
84. K. F. Chiu and S. H. Su, *Thin Solid Films*, 2013, **544**, 144-147.
85. P. Sivaraman, V. R. Hande, V. S. Mishra, C. S. Rao and A. B. Samui, *J. Power Sources*, 2003, **124**, 351-354.
86. P. Sivaraman, R. K. Kushwaha, K. Shashidhara, V. R. Hande, A. P. Thakur, A. B. Samui and M. M. Khandpekar, *Electrochim. Acta*, 2010, **55**, 2451-2456.
87. M. M. Khandpekar, R. K. Kushwaha and S. P. Pati, *Solid-State Electronics*, 2011, **62**, 156-160.
88. P. Sivaraman, S. K. Rath, V. R. Hande, A. P. Thakur, M. Patri and A. B. Samui, *Synth. Met.*, 2006, **156**, 1057-1064.
89. D. Rathod, M. Vijay, N. Islam, R. Kannan, U. Kharul, S. Kurungot and V. Pillai, *J. Appl. Electrochem.*, 2009, **39**, 1097-1103.
90. R. S. Hastak, P. Sivaraman, D. D. Potphode, K. Shashidhara and A. B. Samui, *Electrochim. Acta*, 2012, **59**, 296-303.
91. R. S. Hastak, P. Sivaraman, D. D. Potphode, K. Shashidhara and A. B. Samui, *J. Solid State Electrochem.*, 2012, **16**, 3215-3226.
92. A. J. Polak and P. Young, U. S. Patents, US4714482, U.S., 1987

93. Z. S. Wu, K. Parvez, X. Feng and K. Müllen, *Nat Commun*, 2013, **4**, 1-8.
94. Y. Xu, Z. Lin, X. Huang, Y. Liu, Y. Huang and X. Duan, *ACS Nano*, 2013, **7**, 4042-4049.
95. K. Gao, Z. Shao, X. Wang, Y. Zhang, W. Wang and F. Wang, *RSC Advances*, 2013, **3**, 15058-15064.
96. P. Karthika, N. Rajalakshmi and K. S. Dhathathreyan, *ChemPhysChem*, 2013, **14**, 3822-3826.
97. S. T. Senthilkumar, R. K. Selvan, J. S. Melo and C. Sanjeeviraja, *ACS Appl. Mater. Interfaces*, 2013, **5**, 10541-10550.
98. H. Yu, J. Wu, L. Fan, Y. Lin, K. Xu, Z. Tang, C. Cheng, S. Tang, J. Lin, M. Huang and Z. Lan, *J. Power Sources*, 2012, **198**, 402-407.
99. M. Kaempgen, C. K. Chan, J. Ma, Y. Cui and G. Gruner, *Nano Lett.*, 2009, **9**, 1872-1876.
100. J. J. Yoo, K. Balakrishnan, J. Huang, V. Meunier, B. G. Sumpter, A. Srivastava, M. Conway, A. L. Mohana Reddy, J. Yu, R. Vajtai and P. M. Ajayan, *Nano Lett.*, 2011, **11**, 1423-1427.
101. M. F. El-Kady, V. Strong, S. Dubin and R. B. Kaner, *Science*, 2012, **335**, 1326-1330.
102. X. Chen, L. Qiu, J. Ren, G. Guan, H. Lin, Z. Zhang, P. Chen, Y. Wang and H. Peng, *Adv. Mater.*, 2013, **25**, 6436-6441.
103. M. Morita, J.-L. Qiao, N. Yoshimoto and M. Ishikawa, *Electrochim. Acta*, 2004, **50**, 837-841.
104. D. P. Dubal, G. S. Gund, R. Holze, H. S. Jadhav, C. D. Lokhande and C.-J. Park, *Electrochim. Acta*, 2013, **103**, 103-109.
105. W. Si, C. Yan, Y. Chen, S. Oswald, L. Han and O. G. Schmidt, *Energy Environ. Sci.*, 2013, **6**, 3218-3223.
106. X. Wang, B. Liu, Q. Wang, W. Song, X. Hou, D. Chen, Y.-b. Cheng and G. Shen, *Adv. Mater.*, 2013, **25**, 1479-1486.
107. Z.-S. Wu, A. Winter, L. Chen, Y. Sun, A. Turchanin, X. Feng and K. Müllen, *Adv. Mater.*, 2012, **24**, 5130-5135.
108. C. Meng, C. Liu, L. Chen, C. Hu and S. Fan, *Nano Lett.*, 2010, **10**, 4025-4031.
109. G. Xiong, C. Meng, R. G. Reifenberger, P. P. Irazoqui and T. S. Fisher, *Adv. Energy Mater.*, 2014, **4**, 1300515.
110. B. Anothumakkool, A. Torris A. T, S. N. Bhange, S. M. Unni, M. V. Badiger and S. Kurungot, *ACS Appl. Mater. Interfaces*, 2013, **5**, 13397-13404.
111. K. Wang, W. Zou, B. Quan, A. Yu, H. Wu, P. Jiang and Z. Wei, *Adv. Energy Mater.*, 2011, **1**, 1068-1072.
112. C. Meng, J. Maeng, S. W. M. John and P. P. Irazoqui, *Adv. Energy Mater.*, 2014, **4**, 1301269.
113. K. K. Lian, C. Li, R. H. Jung and J. G. Kincs, U. S. Patents, US5587872, U.S., 1996
114. M. Xue, Z. Xie, L. Zhang, X. Ma, X. Wu, Y. Guo, W. Song, Z. Li and T. Cao, *Nanoscale*, 2011, **3**, 2703-2708.
115. X. Xiao, T. Li, P. Yang, Y. Gao, H. Jin, W. Ni, W. Zhan, X. Zhang, Y. Cao, J. Zhong, L. Gong, W.-C. Yen, W. Mai, J. Chen, K. Huo, Y.-L. Chueh, Z. L. Wang and J. Zhou, *ACS Nano*, 2012, **6**, 9200-9206.

116. L. Yuan, X.-H. Lu, X. Xiao, T. Zhai, J. Dai, F. Zhang, B. Hu, X. Wang, L. Gong, J. Chen, C. Hu, Y. Tong, J. Zhou and Z. L. Wang, *ACS Nano*, 2011, **6**, 656-661.
117. L. Peng, X. Peng, B. Liu, C. Wu, Y. Xie and G. Yu, *Nano Lett.*, 2013, **13**, 2151-2157.
118. J. Tao, N. Liu, W. Ma, L. Ding, L. Li, J. Su and Y. Gao, *Sci. Rep.*, 2013, **3**, 2286.
119. M. Xue, F. Li, J. Zhu, H. Song, M. Zhang and T. Cao, *Adv. Funct. Mater.*, 2012, **22**, 1284-1290.
120. L. Yuan, X. Xiao, T. Ding, J. Zhong, X. Zhang, Y. Shen, B. Hu, Y. Huang, J. Zhou and Z. L. Wang, *Angew. Chem. Int. Ed.*, 2012, **51**, 4934-4938.
121. Q. Liu, O. Nayfeh, M. H. Nayfeh and S.-T. Yau, *Nano Energy*, 2013, **2**, 133-137.
122. H. Wada, K. Yoshikawa, S. Nohara, N. Furukawa, H. Inoue, N. Sugoh, H. Iwasaki and C. Iwakura, *J. Power Sources*, 2006, **159**, 1464-1467.
123. J. Przyłuski, Z. Połtarzewski and W. Wieczorek, *Polymer*, 1998, **39**, 4343-4347.
124. S. Nohara, T. Miura, C. Iwakura and H. Inoue, *Electrochemistry*, 2007, **75**, 579-581.
125. S. Sampath, N. A. Choudhury and A. K. Shukla, *J. Chem. Sci.*, 2009, **121**, 727-734.
126. N. A. Choudhury, A. K. Shukla, S. Sampath and S. Pitchumani, *J. Electrochem. Soc.*, 2006, **153**, A614-A620.
127. S. Yamazaki, A. Takegawa, Y. Kaneko, J.-i. Kadokawa, M. Yamagata and M. Ishikawa, *Electrochem. Commun.*, 2009, **11**, 68-70.
128. I. Stepniak and A. Ciszewski, *Electrochim. Acta*, 2011, **56**, 2477-2482.
129. J. Kalupson, D. Ma, C. A. Randall, R. Rajagopalan and K. Adu, *J. Phys. Chem. C*, 2014, **118**, 2943-2952.
130. K. M. Kim, J. H. Nam, Y.-G. Lee, W. I. Cho and J. M. Ko, *Curr. Appl. Phys.*, 2013, **13**, 1702-1706.
131. M. Aoki, K. Tadanaga and M. Tatsumisago, *Electrochem. Solid-State Lett.*, 2010, **13**, A52-A54.
132. J. M. Ko, R. Y. Song, H. J. Yu, J. W. Yoon, B. G. Min and D. W. Kim, *Electrochim. Acta*, 2004, **50**, 873-876.
133. H.-S. Nam, J. S. Kwon, K. M. Kim, J. M. Ko and J.-D. Kim, *Electrochim. Acta*, 2010, **55**, 7443-7446.
134. F. Moser, L. Athouël, O. Crosnier, F. Favier, D. Bélanger and T. Brousse, *Electrochem. Commun.*, 2009, **11**, 1259-1261.
135. A. Hardwick, P. G. Dickens and R. C. T. Slade, *Solid State Ionics*, 1984, **13**, 345-350.
136. K. D. Kreuer, M. Hampele, K. Dolde and A. Rabenau, *Solid State Ionics*, 1988, **28–30, Part 1**, 589-593.
137. R. C. T. Slade, H. A. Pressman and E. Skou, *Solid State Ionics*, 1990, **38**, 207-211.
138. R. C. T. Slade, J. Barker and H. A. Pressman, *Solid State Ionics*, 1988, **28–30, Part 1**, 594-600.
139. U. B. Mioč, M. R. Todorović, M. Davidović, P. Colomban and I. Holclajtner-Antunović, *Solid State Ionics*, 2005, **176**, 3005-3017.
140. B. Tazi and O. Savadogo, *Electrochim. Acta*, 2000, **45**, 4329-4339.
141. S. Malhotra and R. Datta, *J. Electrochem. Soc.*, 1997, **144**, L23.
142. A. Micek-Ilnicka, *J. Mol. Catal. A: Chem.*, 2009, **308**, 1-14.

143. O. Nakamura, I. Ogino and T. Kodama, *Solid State Ionics*, 1981, **3–4**, 347-351.
144. O. Nakamura, I. Ogino and T. Kodama, *Mater. Res. Bull.*, 1980, **15**, 1049-1054.
145. K. Lian and C. M. Li, *Electrochem. Commun.*, 2009, **11**, 22-24.
146. K. Lian and Q. Tian, *Electrochem. Commun.*, 2010, **12**, 517-519.
147. Q. Tian and K. Lian, *Electrochem. Solid-State Lett.*, 2010, **13**, A4-A6.
148. H. Gao, Q. Tian and K. Lian, *Solid State Ionics*, 2010, **181**, 874-876.
149. H. Gao and K. Lian, *Electrochim. Acta*, 2010, **56**, 122-127.
150. H. Gao and K. Lian, *J. Power Sources*, 2011, **196**, 8855-8857.
151. H. Gao and K. Lian, *J. Electrochem. Soc.*, 2011, **158**, A1371-A1378.
152. T. Dippel, K. D. Kreuer, J. C. Lassègues and D. Rodriguez, *Solid State Ionics*, 1993, **61**, 41-46.
153. K.-D. Kreuer, *Chem. Mater.*, 1996, **8**, 610-641.
154. H. Gao, Y.-J. Ting, N. P. Kherani and K. Lian, *J. Power Sources*, 2013, **222**, 301-304.
155. K. Jost, D. Stenger, C. R. Perez, J. K. McDonough, K. Lian, Y. Gogotsi and G. Dion, *Energy Environ. Sci.*, 2013, **6**, 2698-2705.
156. H. Gao and K. Lian, *J. Electrochem. Soc.*, 2013, **160**, A505-A510.
157. H. Gao and K. Lian, *J. Mater. Chem.*, 2012, **22**, 21272-21278.
158. D. Pech, M. Brunet, H. Durou, P. Huang, V. Mochalin, Y. Gogotsi, P. L. Taberna and P. Simon, *Nature Nanotech.*, 2010, **5**, 651-654.
159. K. Sheng, Y. Sun, C. Li, W. Yuan and G. Shi, *Sci. Rep.*, 2012, **2**, 247.